Development of a Focused Ultrasonic Array System for Pasture Biomass Estimation

MASSEY UNIVERSITY
TE KUNENGA KI PŪREHUROA
UNIVERSITY OF NEW ZEALAND

A thesis presented in fulfilment of the requirements for the degree of

Master of Engineering

at Massey University, Albany, New Zealand.

ZHILIN JIANG

2023

Abstract

The ability to accurately measure pasture biomass can significantly impact the profitability of the pasture agriculture industry. One technique that has been used to estimate pasture biomass is to measure pasture height using ultrasonic transducers. It was traditionally achieved using a single ultrasonic transducer with a wide beam angle. Additionally, the previous studies using this method only used the first arrival time of the echo from the top of the grass. However, this can lead to overestimating grass height due to isolated pieces of grass, which may not be directly below the sensor. It does not measure the pasture density. Also, height measurement errors may occur when the sensor is mounted on an agricultural vehicle as the vehicle bounces and tilts. To solve these problems, Legg and Bradley developed a new ultrasonic air-coupled transducer array to estimate the biomass of pastures and achieved good experimental results. However, it was believable that measurement accuracy can be further improved using near-field focusing of the transmit and receive arrays.

This work describes the development of an ultrasonic array system capable of focusing on the near and far fields for pasture biomass estimation. It extended on the system developed by Legg and Bradley. Angular measurements were made with the array attached to a computer-controlled turntable system for different near- and far-field beamforming configurations. It was found that improved beamwidth and dynamic range were obtained when the system focused on the receiver in the near field. Some initial lab measurements were also performed on pasture samples, comparing the effect of using the array's transmit far-field and near-field focusing. The results indicate that focusing the array in the near field improves the performance in detecting the grass, particularly the top, compared with focusing the receiver in the near field and the transmitter in the far field. However, more work is needed, including field trials.

Acknowledgement

First and most importantly, I thank my supervisor, Dr. Mathew Legg, for his care and guidance during my graduate studies. His rigorous, meticulous academic style and persuasive and eclectic teaching style have deeply influenced me and made me proud of him. I keep making progress and pursuing academics hard. Thanks to Mr Kartikay Lal for his selfless education on experimental equipment and application software. These are essential factors for the smooth completion of my graduation thesis. Thanks to Dr Rezaul Hasan, Dr Frazer Noble, Dr Khalid Arif and other theoretical teachers for their hard work. Their teaching content is the source of ideas for my graduation thesis. Thanks to Professor Fakhrul Alam, who has contributed a lot to the development of our college. Accessing materials is undoubtedly an essential part of graduate study. I want to thank the teachers in Massey Library for their selfless help during this process. The experiments for this thesis were conducted at Massey University, and I would like to thank the university leaders for their support.

I want to thank my classmate Yinxuan Hu, who greatly encouraged me when I was frustrated and hesitant. Without his help, I would not have been able to complete my studies.

I would also like to thank my family, my parents, my children, and especially my wife, Ying Jiang, who cared for my little son and older people at home while I was studying for my master's degree. For such great mental and material support, a word of thank you cannot express the guilt and gratitude I feel in my heart.

Outline

1. Introduction

Farm productivity is closely related to the ability to predict crop yields accurately. Take pasture as an example. It can usually be cut from an area, dried, and weighed to estimate the yield per unit area of the entire pasture. Due to the low sampling area, this method is destructive to pasture crops, time-consuming, and unlikely to provide representative information. Therefore, this method is generally only used to compare with other techniques in detail and is not a practical option for everyday use by farmers. Methods currently used to estimate pasture biomass include measuring parameters such as capacitance, optical reflectance spectral characteristics (Hardisky, Smart, & Klemas, 1983), pasture height where the extension of the light is implemented (Milsom et al., 2019), and compressed turf height where the record changes in pasture compressibility to assess pasture growth and development (Earle & McGowan, 1979; Lush, 1990). Various optical sensors have been used in remote sensing measurements (Reusch, 2009). Satellite remote sensing technology is also commonly used (Ahamed, Tian, Zhang, & Ting, 2011; Ali, Cawkwell, Dwyer, & Green, 2016). However, in actual measurements, for farmers, the accuracy of remote sensing technology still needs to be improved, for the thickness of the cloud affects the results of pasture biomass. It has been reported that satellite remote sensing has the potential to measure farm biomass accurately, but longer-term research is needed to refine it (Akhtar et al., 2020; Gargiulo et al., 2023; Kumar & Mutanga, 2017). Therefore, there is still a need for close-range (proximal) sensing technologies for measuring biomass that can provide farmers with more accurate and real-time data with higher special resolution that can complement satellite remote sensing technology (Adamchuk, Rossel, Sudduth, & Lammers, 2011; Brisco, Brown, Hirose, McNairn, & Staenz, 1998; Liu, Bruning, Garnett, & Berger, 2020; Wachendorf, Fricke, & Möckel, 2018; White et al., 2012). Proximity sensing technology generally uses air-coupled ultrasonic sensors in an array arrangement, which has very obvious advantages compared with a single sensor arrangement(Allevato et al., 2022; Dworak, Selbeck, & Ehlert, 2011; Legg & Bradley, 2019b; Omia et al., 2023). It can provide higher resolution and easier-to-receive signals, and the area covered by the signal is also significantly wider. The role of ultrasonic arrays in actual measurement will be introduced in the following sections.

1.1 Ultrasonic pasture biomass estimation

The ultrasonic technique has been utilised in the pasture biomass estimation field as one of the non-detractive techniques. Generally, the sensor emits ultrasonic waves toward the ground. The

ultrasonic waves return to the sensor after being reflected off the blades of grass. The measured time of the first echo and the speed of sound allows the distance between the top of the grass and the sensor to be measured. If the height of the sensor above the ground surface is known, the height of the pasture can be measured and used to estimate pasture biomass. The first work that used ultrasonic waves to measure pasture height for biomass estimation was by Hutchings et al. (Hutchings, Phillips, & Dobson, 1990). They installed the transducer on an aluminium stick, inserted one end into the ground, then picked up the metal stick and changed to the next position after the transducer completed transmitting and receiving signals. However, this method requires manual operation and has a limited measurement area. In order not to manually change the position, it seems more suitable to install the transducer on a motorbike or farm vehicle.

The ultrasonic transducer is mounted onto the back of a farm vehicle, emitting ultrasonic waves to detect the top of the grass below the farm vehicle. However, since the land is not flat, there are bumps during the driving, and errors in height measurement are inevitable, particularly if the weight distribution changes, such as a dog jumping on the back. The ultrasonic transducer can also be installed in front, behind the vehicle, or on the side (Enterprises, 2023). Additionally, this system can't detect variations in pasture density.

Some studies combine hyperspectral techniques and ultrasonic techniques to find more information, including the height and density of the grass, to figure out how to estimate the pasture biomass more accurately (Fricke & Wachendorf, 2013). It is also noticed that in previous articles related to measuring pasture biomass, they generally only mentioned that the first echo returned from the top of the blade of grass was measured, which is enough to measure the height from the transducer to the grass. However, the echo from the ground is not used, which means they can't get the situation of the ground.

To overcome these issues, Legg and Bradley developed a low-frequency ultrasonic sensor system with a narrow beamwidth and higher temporal resolution for proximal range pasture measurements (Legg & Bradley, 2019c). They used low ultrasonic frequencies (<40 kHz) to provide good penetration through the grass to the ground. Unlike previous work, they did not only use the first echo time from the top of the blade of grass and soil but echoes from a range of distances. It allowed the ground location to be measured and appeared to allow pasture density to be estimated. This article is a continuation of that research.

1.2 Low-frequency ultrasonic transducer array

A single low-frequency air-coupled ultrasonic transducer has poor depth resolution with wide beam width and long pulse duration compared with a high-frequency air-coupled ultrasonic transducer (Akhbari, Sammoura, Eovino, Yang, & Lin, 2016; Gomez Alvarez-Arenas, 2017; Kažys, Vladišauskas, & Žukauskas, 2004). Various works have investigated using ultrasonic transducer arrays to overcome this weakness. Ahmad et al. researched phased arrays of multiple transducers (Ahmad, Kundu, & Placko, 2005). When each transducer with a broader beam angle is placed in a phased array, a more focused and narrower beam can be produced (Xiong, He, & Peng, 2020). At the same time, to avoid special aliasing (grading lobes), the minimum distance between the transducers should be less than half of the wavelength λ of the emitted sound wave (Paul, Barthez, Léveillé, Peter, & Scrivani, 1997). For a set of transducers operating at 20kHz, the distance between them should be approximately 9mm. Minimum transducer spacing greater than this results in undesirable spatial aliasing in multiple grating lobes (Harput & Bozkurt, 2008). Unlike ordinary, spiral array configurations are more feasible as they require fewer array elements (Price & Long, 2018). The spiral array configurations can reduce the use of components while still ensuring high-quality resolution. The beam pattern diagram at a fixed frequency is shown in Figure 1:

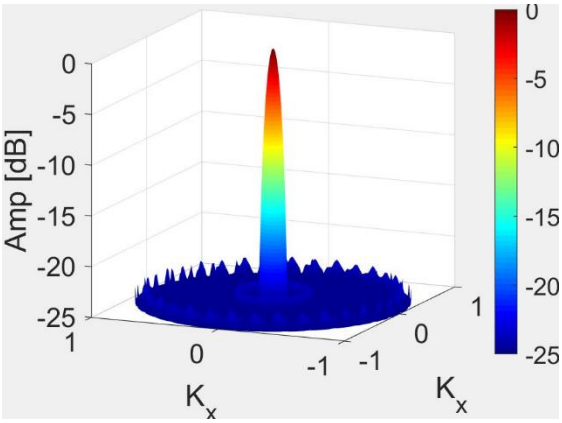

Figure 1 The beam pattern diagram of a spiral transducer array (Legg & Bradley, 2019a).

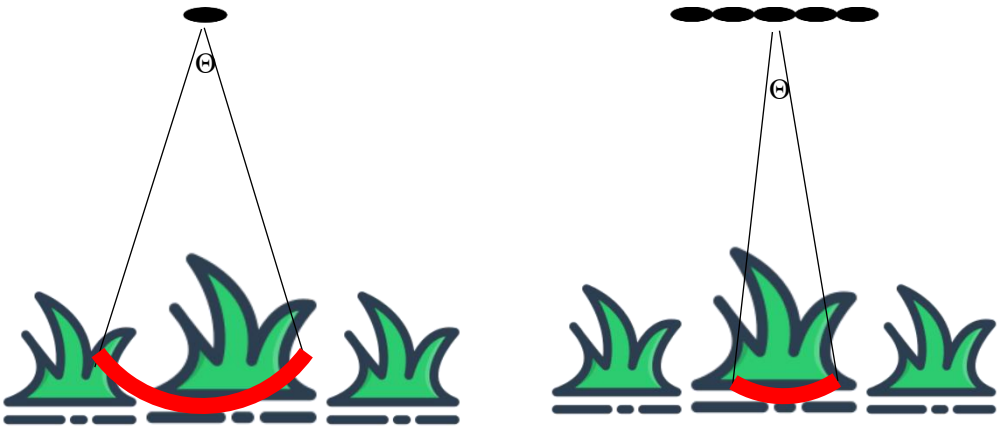

(a) A single or a small number of transducers can obtain a wide scanning area and low resolution.

(b)Transducer array can focus on narrow area and get high resolution.

Figure 2 The difference between single transducer and transducer array when it focuses on the echo from the ground.

Legg and Bradley developed a low-frequency air-coupled ultrasonic transducer array to measure pasture biomass, allowing narrower beamwidth and higher depth resolution than a single transducer (Legg & Bradley, 2019b). Figure 2 shows the work reduces echoes from stray grass pieces to the side and allows profiling through the pasture to the ground to measure pasture height and estimate grass density. It contrasts with previous work works that had only used the first echo from the top of blades of grass. They used low ultrasonic frequencies as they believed this would allow profiling down through the pasture depth to the ground better than higher ultrasonic frequencies.

They developed two versions of their array system. One was more commercial, with fixed beamwidth focusing on the far-field. Another research version was developed that could have different beam widths and was also used for far-field focusing. Although this was not used in their work, the system could focus on the near field for the reception but not on transmission.

The following section introduces the original ultrasonic pasture estimation array system and how this system was used to obtain pasture measurements in the field.

1.3 Original pasture biomass estimation system developed by Legg and Bradley

The ultrasonic transducer array and reception system were developed to investigate the effect of using different beam widths and numbers of transducers and microphones on pasture biomass estimation (Legg & Bradley, 2020). However, this version was a research tool not viewed as a potential commercial product. The signal generation and reception transducers are

204 MEMS microphones and 160 Murata MA40H1S-R surface mount transducers. The MEMS microphones could detect ultrasonic frequencies. The Murata MA40H1S-R transducers were chosen due to their small size and low ringing.

1.3.1 Transducer ringing effects

Ultrasonic biomass estimation has traditionally used air-coupled sensors designed for finding distance. These types of transducers have a resonant frequency at which they have maximum gain. However, the transducers tend to "ringing" at this resonance frequency. It is okay if one wishes to find the closest object (such as the top of the grass) as one is only using the first

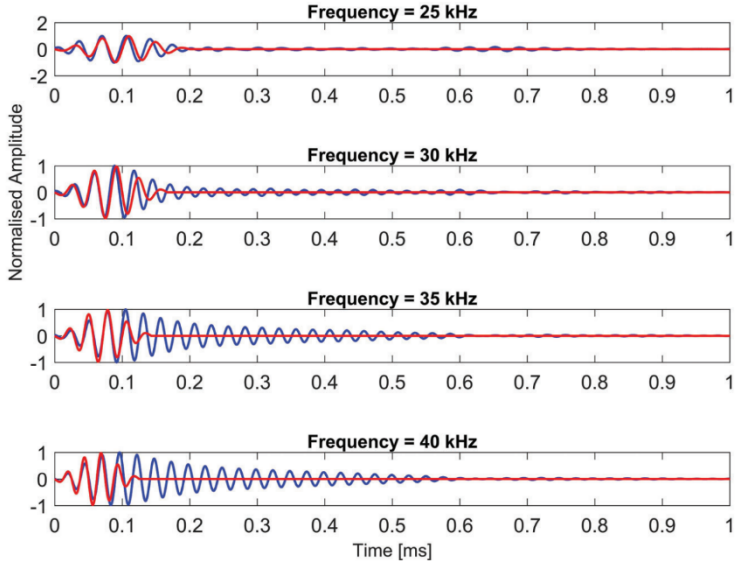

(a) Transducer ringing at different frequency.

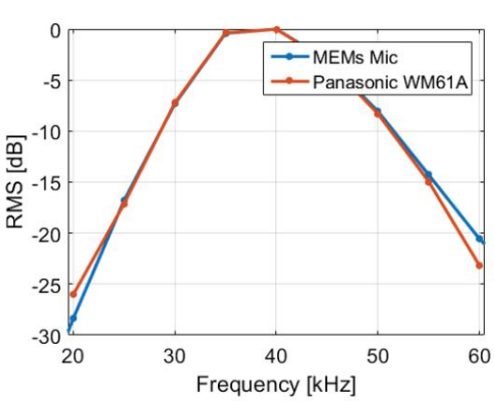

(b) The gain reduces when frequency goes away from resonant frequency of 40 kHz.

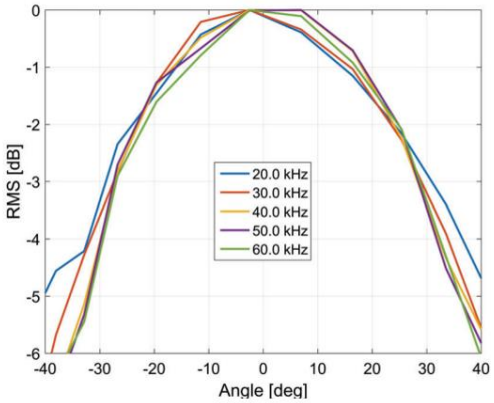

(c) The gain reduces when the transducer turns to different angles.

Figure 3 Single transducer frequency and angular response. Overlaid in red is the signal applied to the transducer (Legg & Bradley, 2019b).

arrival time. However, for the work performed by Legg and Bradley (Legg & Bradley, 2019b), they wanted to analyse echoes from the top of the grass down to the ground. In this case, ringing of the transducers is undesirable. When they ring, the received echo signal from different depths within the grass becomes indistinguishable, leading to poor depth resolution.

Figure 3(a) shows examples of the transducer ringing used in this work for different transmit frequencies. The ringing effect is reduced when the emission frequency is either lower or higher than the resonant frequency of 40 kHz. But at the same time, Figure 3(b)(c) shows the gain is reduced if one transmits at frequencies away from the resonance frequency or changing angles. Legg and Bradley, therefore, used transmitting frequencies away from the resonance (20-25 and 55-60 kHz) to ensure transmission with minimal ringing (Legg & Bradley, 2019b). It reduced the gain relative to the resonance frequency of 40 kHz. However, this reduced gain was not an issue because the array has many transducers.

1.3.2 Transmission and Reception Array

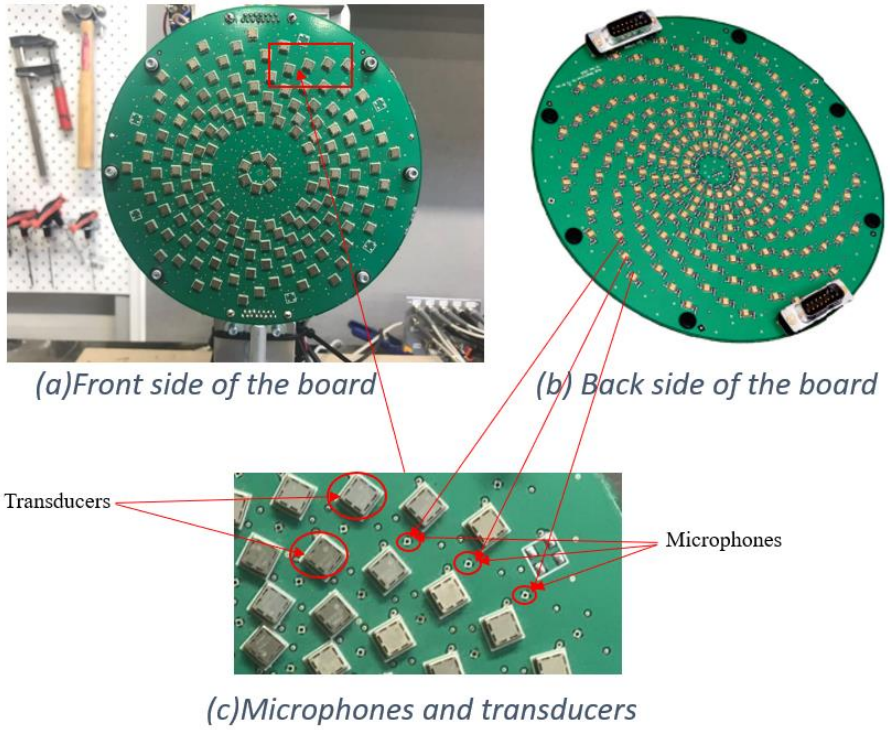

Figure 4 Transmitting and reception PCB board.

Figure 4 shows the transmitting and receiving PCB board. Both the transmit and receiver arrays of the board are based on a 17-arm multi-arm spiral. The receiver array consists of 12 rings, each containing 17 microphones. For each ring, the signal from all the microphones in the ring is combined using a summing preamplifier, and the output goes through to one of the 12 ADC channels on the DT9836 board referred to in Figure 5:

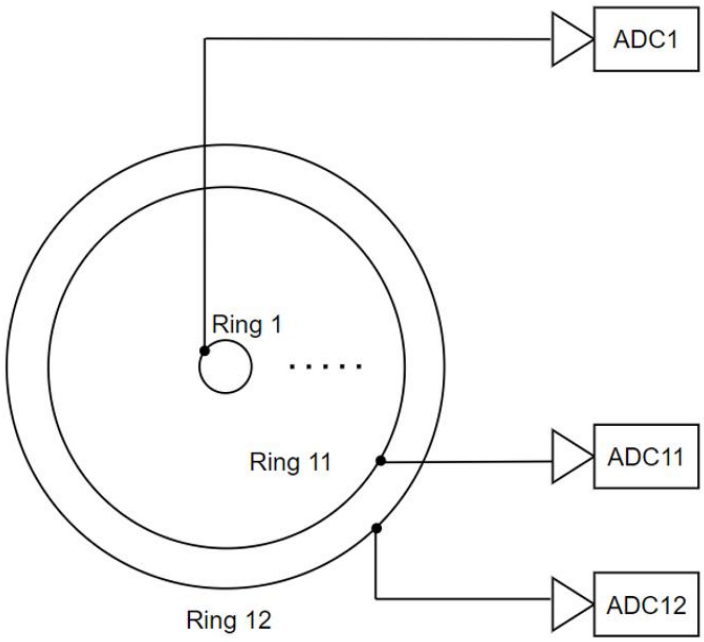

Figure 5 Simplified diagram of how an individual ADC channel is used for each microphone ring in reception.

Likewise, there are 10 transmitter rings. The outer 9 rings contain 17 transducers, while the inner transmitter ring contains 7. The transducers in each ring are connected in parallel and driven by one of the two power supplies via a relay Amplifier/DAC channel of the DT9836 board. A digital output DT9836 board controlled the relays. Figure 6 is the configuration diagram (Legg & Bradley, 2019b).

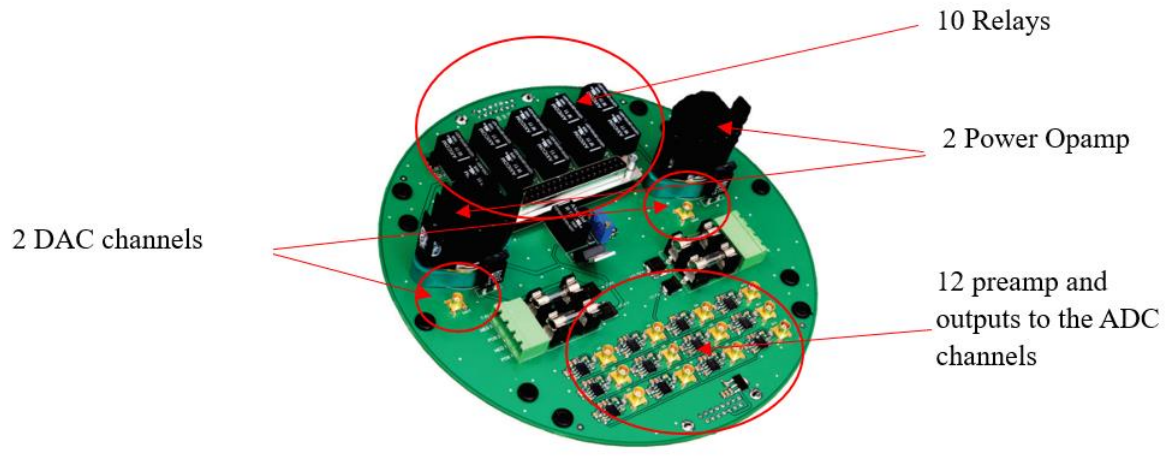

Figure 6 Amplifier printed circuit board (PCB) board.

The ultrasonic array PCB board is plugged into the Amplifier board, which has ten relays connected to 2 power amplifiers and DAC channels, controlled using 10 digital output channels of the DT9836 board referred to in Figure 7:

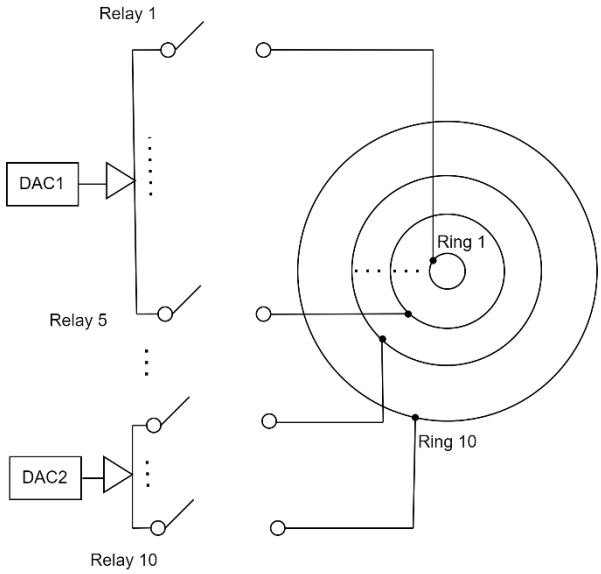

Figure 7 Simplified diagram of how the relays is used to control the 10 transmitting rings. This allowed each transmit ring to be turned on or off independently. Beamforming in the far-field could be achieved by outputting the same signal each of the two DAC channels and using the relays to apply this signal to all 10 transducer channels (5 channels for each DAC).

1.3.3 Pasture measurements using the original array

Pasture biomass was estimated by Legg and Bradley using the array from measured pasture height and estimated pasture density. Figure 8 shows the array was mounted on a farm vehicle

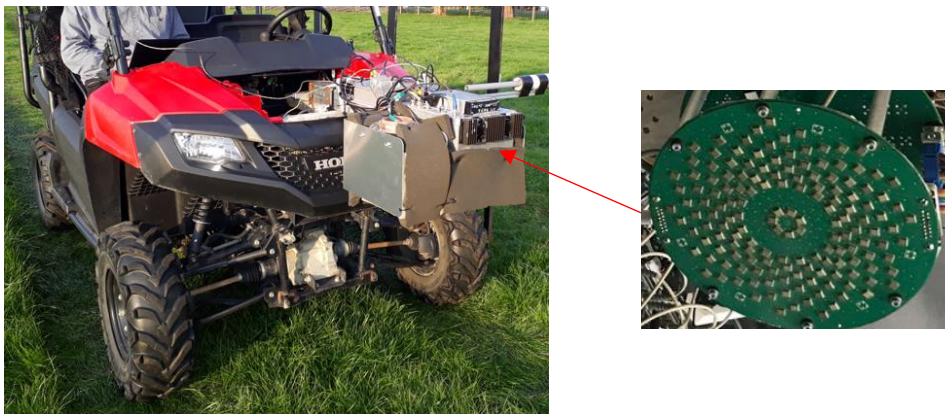

Figure 8 Legg drove a farm vehicle with the array to measure the pasture height in a wild field.

about 700 mm above the ground. Pasture height required the location of the top of the grass and the ground to be estimated. They use 5 cycles of sine waves or linear chirps (25 – 35 kHz) as the transmitting signals. Figure 9 shows improved depth resolution achieved by cross-correlation of the transmit signal with the received echo signals. The green dotted line shows the ground's position, chosen as the highest peak in the cross-correlation signal. The red dotted

line shows the position of the assumed top of the grass, taken as the point when the received cross-correlation signal first went above a threshold.

Additionally, the signal between was analysed to estimate pasture density. The ground location appeared to be detected relatively robustly. However, detection of the top of the grass was felt to be more challenging.

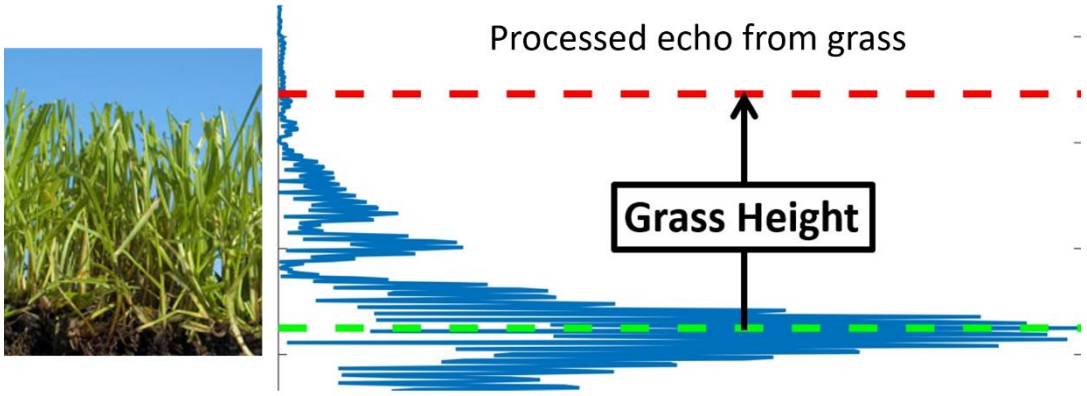

Figure 9 Illustration of how the position of the ground and the first echo from the top of grass was obtained from original system (Legg & Bradley, 2019b).

1.4 Objective of this study

Legg and Bradley only performed measurements focusing on the transmission and reception in the far field (focused on a point at an infinite distance) (Legg & Bradley, 2019b). It was achieved by transmitting the same signal on all transducer rings and then summing the received signal on all microphone receiver rings. Their design could have allowed near-field focusing on reception using beamforming. However, this could not have been performed for transmission. Could improved performance have been achieved by using near-field focusing? By focusing the array in the near-field, a narrower beamwidth and improved depth resolution using cross-correlation could theoretically be achieved. It is believed that this might allow the array to be moved closer to the grass surface, provide an improved ability to detect the location of the top of the grass and ground, and potentially improve the estimation of pasture density.

1.4.1 Scope of Study

This work develops hardware and software based on the original system to improve the transmitting system, allowing the focusing of the array in the near field while keeping the

original reception system hardware unchanged. Code is then developed to allow the newly developed system to focus independently on the transmission and reception in the near or far field as required.

The system is mounted onto a turntable to measure the beam pattern. MATLAB code controls transmission and reception to focus near field or far field respectively or simultaneously and compare the obtained beam pattern curves.

Initial pasture sample experiments are also implemented to investigate if improved performance can be achieved by focusing the transmitting and receiving array in the near field (as opposed to the far field). It is believed that this could improve the system's ability to find the top of the grass and the ground and potentially pasture density measurements.

The beamforming technology is illustrated in Section 2. The hardware of the upgraded system is introduced in Section 3. The lab trial for comparing the effect of using far and near fields focusing on the beamwidth of the array is presented in Section 4. Section 5 provides some initial experiments using the array of pasture samples. Conclusions and future work are in Section 6. Following this, the MATLAB code used is presented in Appendix A and B.

2. Proposed New System

The transmitting and receiving array developed by Legg and Bradley can focus on near-field or at a distance of infinity. When the array needs to focus on the near field, they could have used beamforming technology to focus the reception array on the near field. However, due to the time limitations of the project, this was not done. The transmitting array could not focus in the near field. Theoretically, transmission and reception focusing near-field could improve performance rather than only the reception focusing on near-field. Therefore, a new system using beamforming to focus transmitting and receiving array on near-field is developed in this work.

2.1 Beamforming technology

Beamforming technology has a long history and has been studied in many fields, such as radar, sonar, seismology, and communications. This technology is also the core technology of the transducer array (You, Cretu, Rohling, & Cai, 2011). It can be used for many different purposes, such as detecting the presence of a signal, estimating the direction of arrival (DOA), and enhancing the desired signal (Chen, Yao, & Hudson, 2002; Erdogan, Hershey, Watanabe, Mandel, & Le Roux, 2016; Hamid, Qamar, & Waqas, 2014). Beamformers are generally designed as spatial filters that operate on the output of the transducer array to form the desired beam (Buckley, 1987; Nordebo, Claesson, & Nordholm, 1994; Qian et al., 2018; Van Veen & Buckley, 1988).

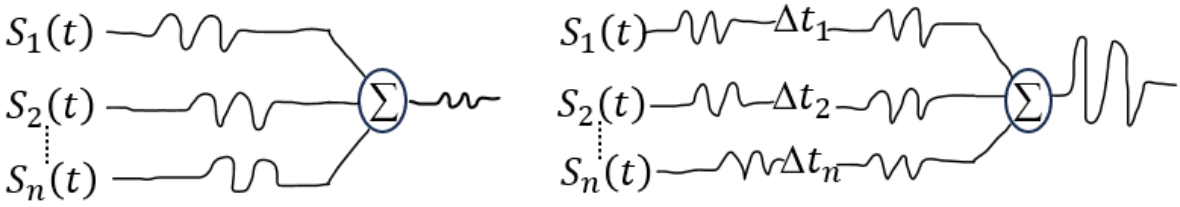

(a) The source signals have different phases, and the intensity of the waveform obtained after superposition may be weaker than the source signal.

(b) The source signals have the same phase after delay processing, and a stronger signal waveform can be obtained after superposition.

Figure 10 Simplified diagram illustrates delay and sum processing of beamforming.

Figure 10(a)(b) shows the simplified beamforming processing. The spatial filtering operation can be further decomposed into two processes: synchronisation and weighted summation. The synchronisation process is to delay (or advance) the output of each transducer by an appropriate amount of time to synchronise the signal components coming from the desired direction. In this step, you need to know the time difference between each transducer transmitting or receiving signals, which can be calculated based on the locations of the transducer array

elements and the speed of the sound wave. Another weighted summation step weights the synchronised signals and adds the results together to form an output (Matrone, Ramalli, D'hooge, Tortoli, & Magenes, 2019). In this step, the average value of the component signals is generally processed. (Note that beamforming can also be performed in the frequency domain, as is discussed later in the text.)

2.2 Reception system for focus in the near field

The original system uses beamforming in the far field by summing up the 12 receiver channels. It was believed that focusing reception on the near field could have improved the system's accuracy. The current system could have achieved this since each microphone ring was connected to a different ADC channel. However, this was not investigated due to the project's time constraints. The following section describes how this could have been achieved.

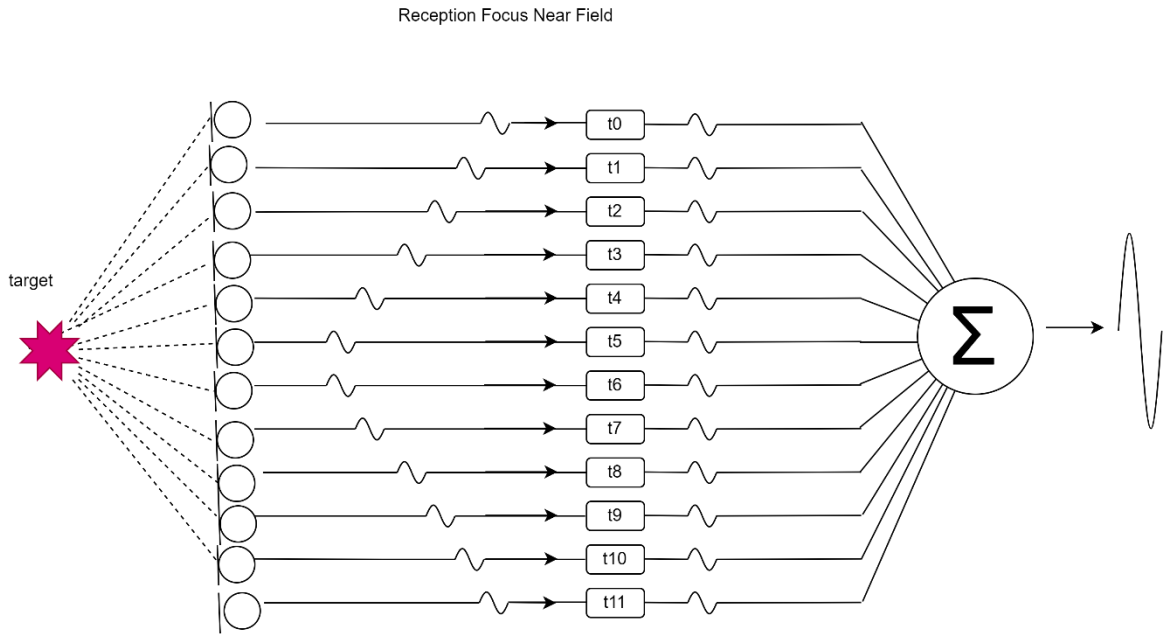

Figure 11 Reception signals focusing near field (RX near).

The original receiver hardware was not changed as it was already capable of near-field beamforming. The software was developed to allow beamforming to focus the array in either near or far field.

There are 12 channels receiving signals, which have been stored in the DT9836 board. When the sound echo from an object in the near field returns to the receiving array, due to the different

lengths of the path, the phase of the sound wave is different for each channel referred to in Figure 11.

The reception signals can be delayed on each of the 12 receiving channels. It can then be averaged to obtain a single channel. The receiving signals matrix [N × M] can be converted to a [1 × M] array using:

$$x\{ n \} = \frac{1}{M} \sum_{m=1}^{M} x_m[index - N_n] \quad (5)$$

where the M is the number of receiving channels. As discussed later, it is also possible to perform the beamforming in the frequency domain.

2.3 Upgraded Transmission system

The original hardware configuration did not allow the focusing of the ultrasonic transmission in the near field using beamforming. It would have required each channel to have a different time delay version of the transmit signal. It would have required an independent DAC channel for each transmitter ring.

To focus the transmission on the near field using beamforming, the system needed to be upgraded to have 10 independent DAC channels at the transmitter to ensure that the 10 ring channels signals of the transmitter can be independently beamformed.

There are two options to upgrade the system to allow the array to focus the ultrasound transmission on the near field using beamforming.

1) Use 10 DAC channels without any power amplifiers for the transmitters.
2) Use 10 independent DAC channels and 10 corresponding power amplifiers for transmission.

The boards planned for the DAC channels were the DT9836 and DT9832A boards. Each DAC channel was believed to have enough power to drive a single transmitter ring without a power amplifier. However, this needed to be verified.

A schematic diagram of the upgraded transmitting system is as follows in Figure 12:

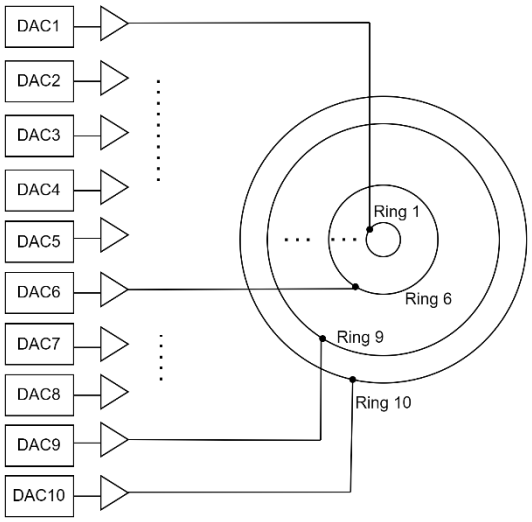

Figure 12 Simplified diagram of how 10 DACs with power amplifiers connect to 10 transmitter rings of the array.

There are 2 DAC channels on each of the DT9836 and DT9832A boards. Hence, 5 boards would be needed to form our DAC channels. In addition, 10 amplifiers need to be formed to complete the construction of the system.

2.3.1 Transmission focusing near field

The beamforming contains 'delay' and 'sum' concepts, which delay the phases of the waveforms to make the waveform signal reach the target at the same time or at different times and can sum the same phase waveform into a high amplitude waveform.

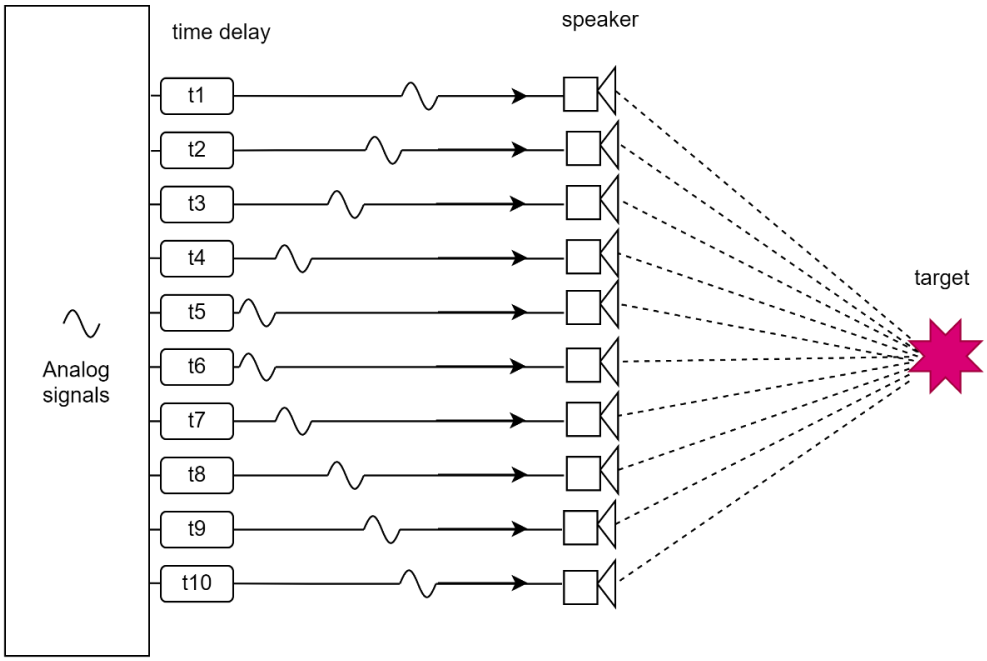

Figure 13 Diagram of the transmitting signals focusing near field (TX near).

Figure 13 illustrates the concept of 'delay'. The signals of 10 channels transmit at the same time, but the transmitted signal cannot reach the target position at the same time. To eliminate this time difference, the Δt_n should be calculated:

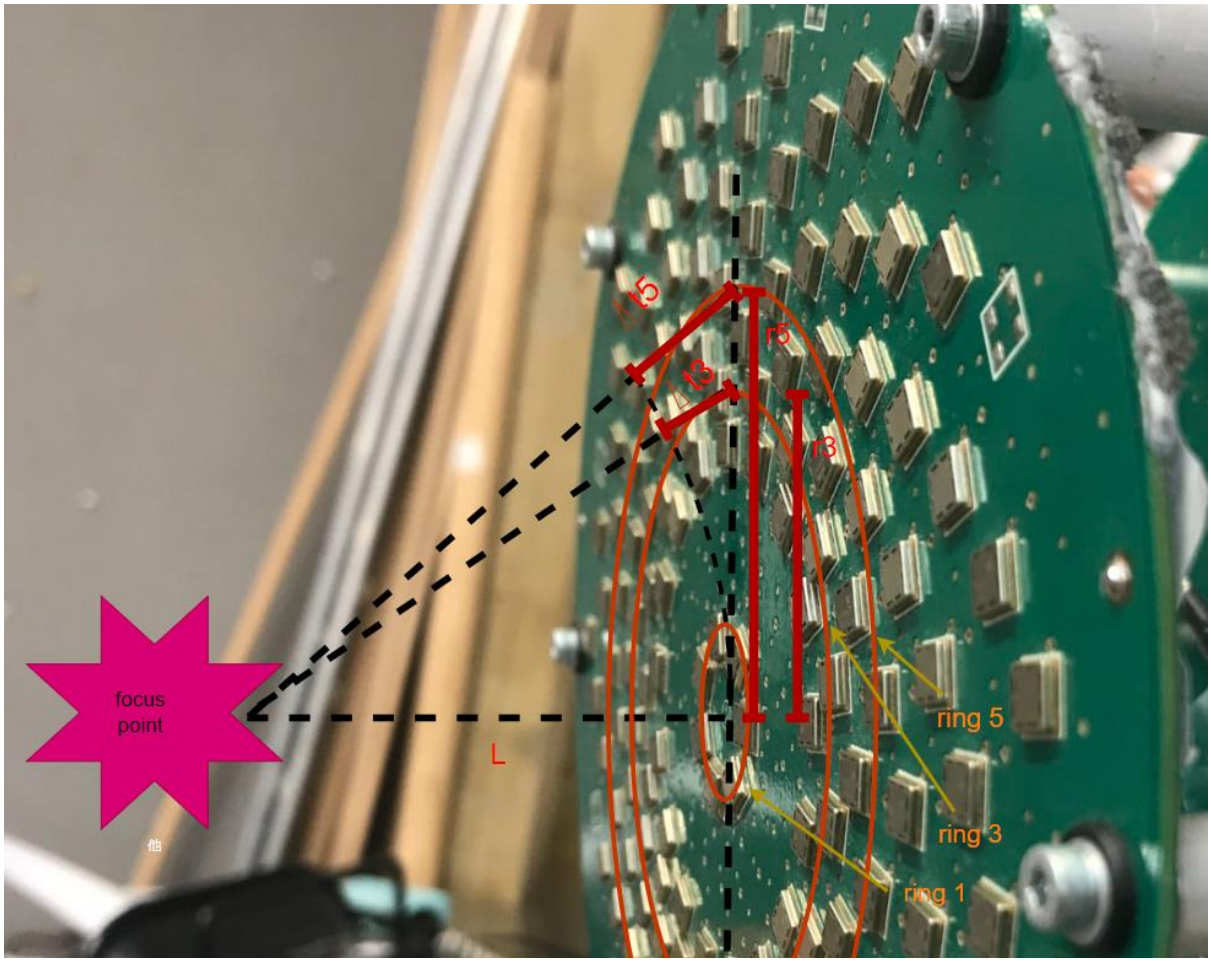

Figure 14 How time delay is calculated for different rings.

Figure 14 shows the relationship between each channel. The signal transmits simultaneously from the transducers to the focus point. The Δt_n stands for the time delay compared with ring 1. The distance between the ring 1 and the target is L, and the distance between CH_1 and CH_n is r_n, assuming that the sound wave velocity is C, then it can calculate the Δt_n :

$$\Delta t_n = (\sqrt{r_n^2 + L^2} - L) / C \quad (1)$$

At the same time, the emission frequency of the signal source is f_s, so the number of sound samples emitted during this time is:

$$N_n = round(\Delta t_n \times f_s) \quad (2)$$

In this way, it only needs to delay N_n samples from each channel can make the signals focus on the near field. The signals in DT9836 and DT9832A boards are stored as an N × M matrix.

N is the number of transmitting samples. For 10 channels, there is a $N_n \times 10$ matrix, which stands for the 10 channels signals. Then, the focusing in near-field signals matrix x$\{ n \}$ can be converted to the below formula:

$$x \{ n \} = x_n(index - N_n) \tag{3}$$

The index equals the length of the signal samples.

There may be a problem when using time domain beamforming because the delays must be multiple sampling intervals, see Equation (3). It means that the sampling rate should be high, or the focus may not be accurate. The frequency domain beamforming technique can be implemented to shift a single transmitting signal by using the following:

$$X_s(\omega, N_n) = X(\omega)e^{\{-i\omega N_n\}} \tag{4}$$

where X is the complex discrete Fourier transform of the signal, and ω is the angular frequencies.

3. Hardware

3.1 Reception system

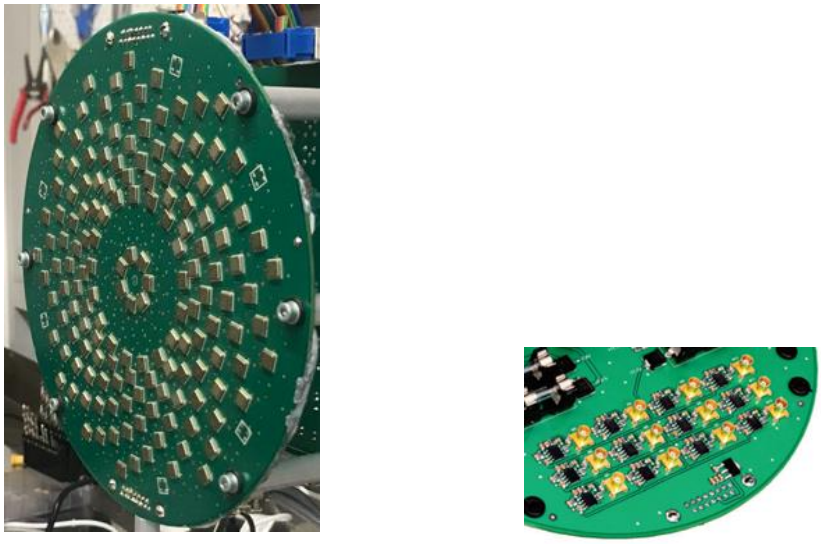

Figure 15 Microphone array and 12 ADC channels with pre-amplifiers.

The reception system hardware was retained from the original system. Figure 15 shows the array and the preamps used for 12 channels of microphone pre-amplifiers (one for each microphone ring), which were connected to the 12 ADC channels of a single DT8936 board. These were not changed from the original system except for some cabling.

Figure 17 illustrates how the received signals pass to a single DT9836 board. Figure 16 shows a single DT9836 board. Table 1 describes the parameters of this board.

Figure 16 Single DT9836 board for reception. Two Analog output channels and twelve Analog input channels will be used in this board.

Table 1 Key features of Data Translation DT9836 for reception

Analog input DT9836					
Channels	Resolution	Max sample rate	Sampling	Ranges	Isolation
Up to 12	16-bit	225 kS/s/ch	Simultaneous	±10 V, ±5 V	±500 V ch-ground

Table 1 shows the DT9836 board has 12 Analog input connectors where the signals received by 12 microphone rings pass. The signals stored in the DT9836 board can perform beamforming for each ring channel, focusing near-field.

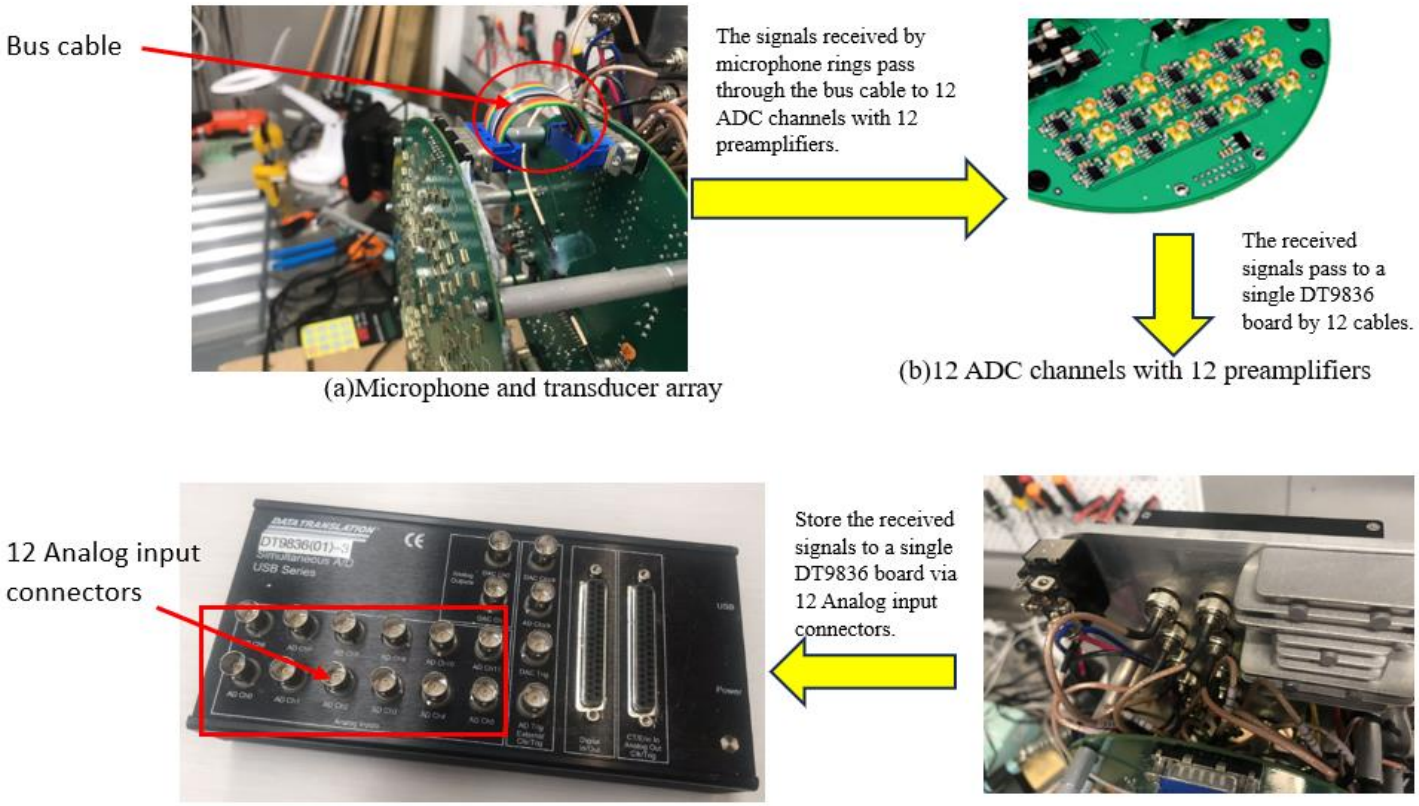

Figure 17 Illustrate the flouncy of how the receiving signals pass to the DT9836 and DT9832A board.

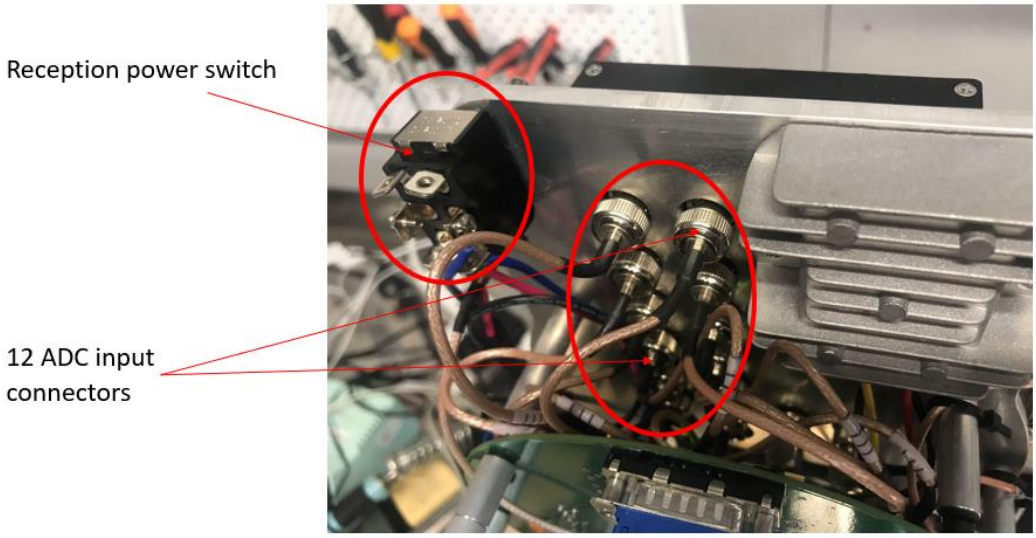

Figure 18 Store the received signals to a single DT9836 board via 12 Analog input connectors.

Figure 18 shows the first DT9836 board is mounted onto the transmitting and reception system. However, there is not enough space to connect the transmitter cables directly. The two PCBs were, therefore, mounted further apart, and the reception plugs were connected using a custom ribbon cable referred to in Figure 19.

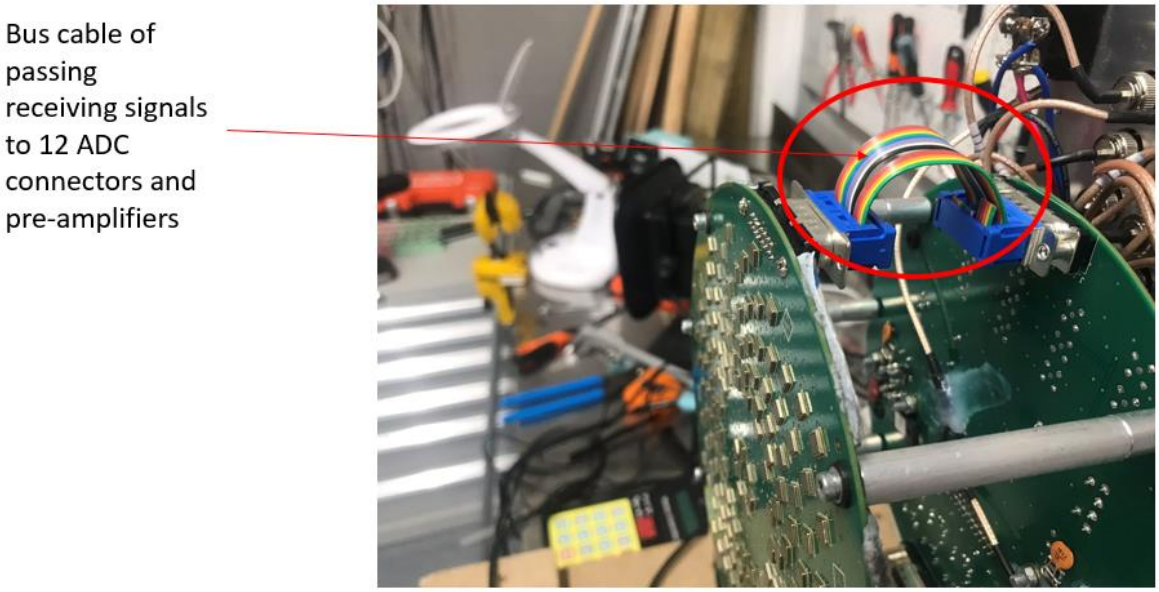

Figure 19 Bus cable connects the microphone array and the back PCB board, which has 12 ADC channels and pre-amplifiers.

The 12 input reception signal connectors receive signals from 12 microphones. The reception power switch controls the power of the reception units when the buttery is connected to the reception system.

The connection bus cable was used to transmit the receiving signals to the reception board.

Figure 20 Two rechargeable batteries rated at 12 volts.

Figure 20 shows the 12 pre-amplifiers work under 24 rate volts, and two rechargeable batteries are necessary to connect them. Each of the batteries has 12 rate volts.

3.2 Upgraded transmission system

(a)Transducer and microphone array (b)One isolated DT9836 board which is mounted with main structure. (c)Four DT9836 and DT9832A boards

Figure 21 Totally 5 DT9836 and DT9832A boards and transducer array which formed upgraded transmission system.

Figure 21 (a)(b)(c) shows the upgraded transmission system has 3 DT9836 boards and 2 DT9832A boards. The DT9836 and boards DT9832A both had 2 analogue outputs each. It gives 10 Analog output channels matched up with the 10 transducer rings. Note that the Amplifier PCB board's original power amplifier and relay part developed by Legg and Bradley were unused. Instead, a cable connected the transmitter array board to the new DAC channel system (with or without power amplifiers) was used.

Figure 22 Connection cable.

Figure 22 shows a connection cable fabricated to connect the 10 DAC channels to the transmitting array.

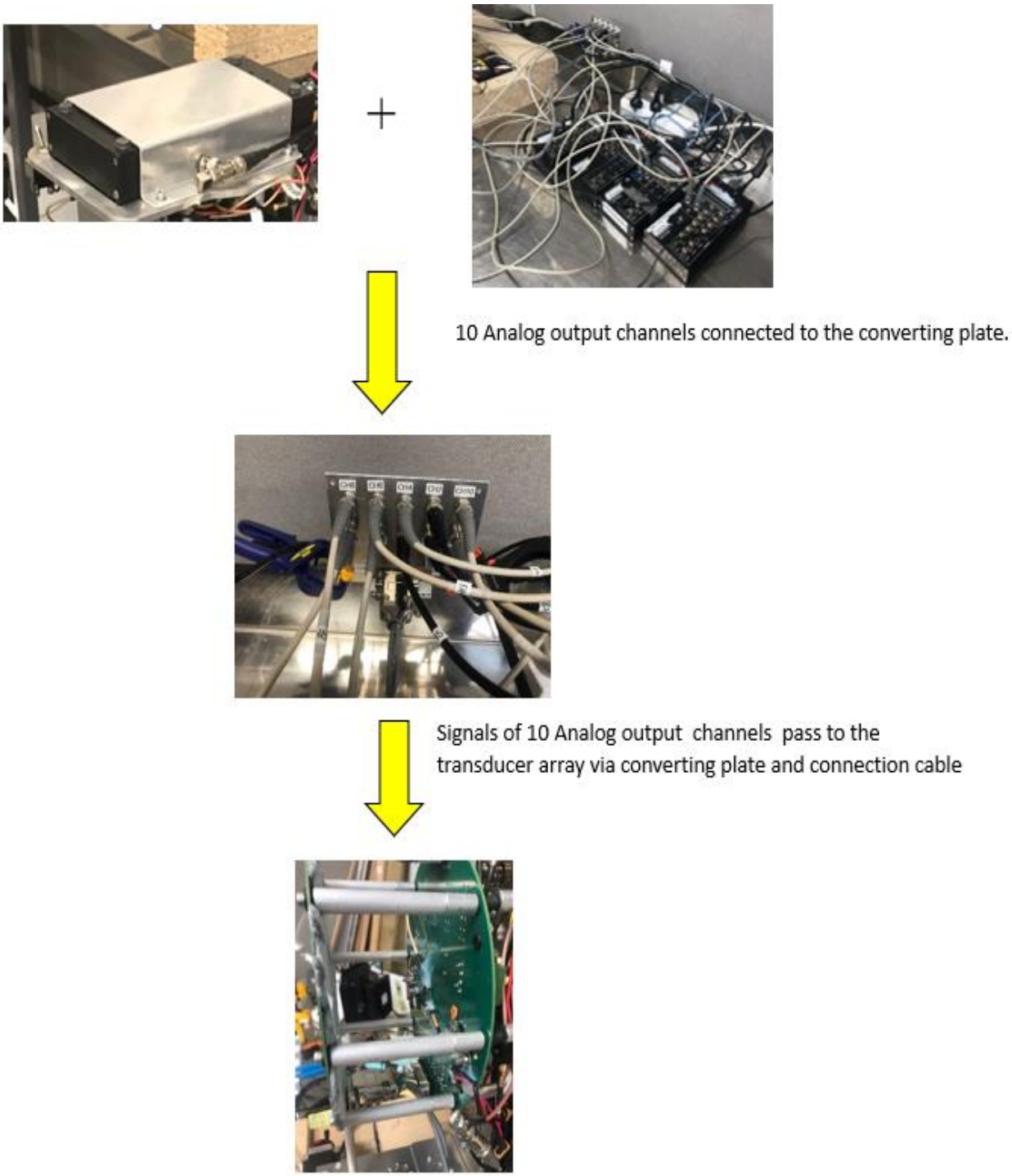

Figure 23 The fluency of how the transmitting signals passing from 10 Analog output channels to the transducer array.

Figure 23 illustrates the fluency of the transmitting signals passing through from 10 Analog output channels to the transmitting array.

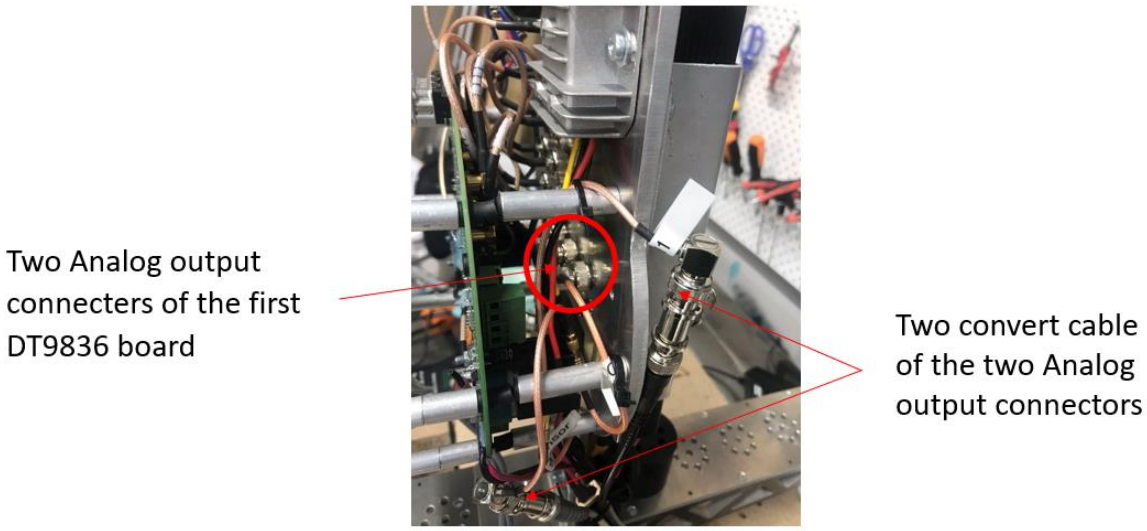

Figure 24. The two Analog output of the first DT9836 board.

As Figure 24 and Figure 25 show, 5 DT9836 and DT9832A boards have been set up to form 10 DAC channels.

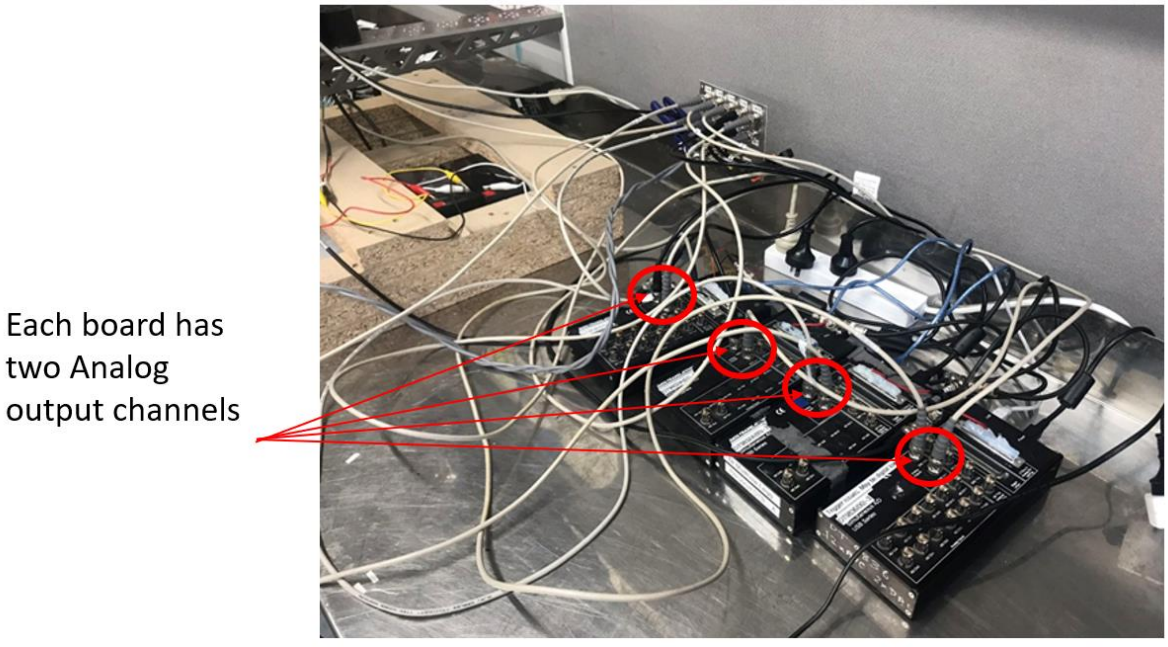

Figure 25 4 DT9836 and DT9832A board, each of them has two Analog output channels.

Figure 26 10 Analog output channels connected to a convert plate which has 10 BNC connectors. The transmitting signals will pass to the transmitting array via connection cable.

Plug 10 channels transmitting CNC cables into a metal plate, which can covertly make the 10 channels signals transmit to the transducers via the connection cable in Figure 26 and Figure 27.

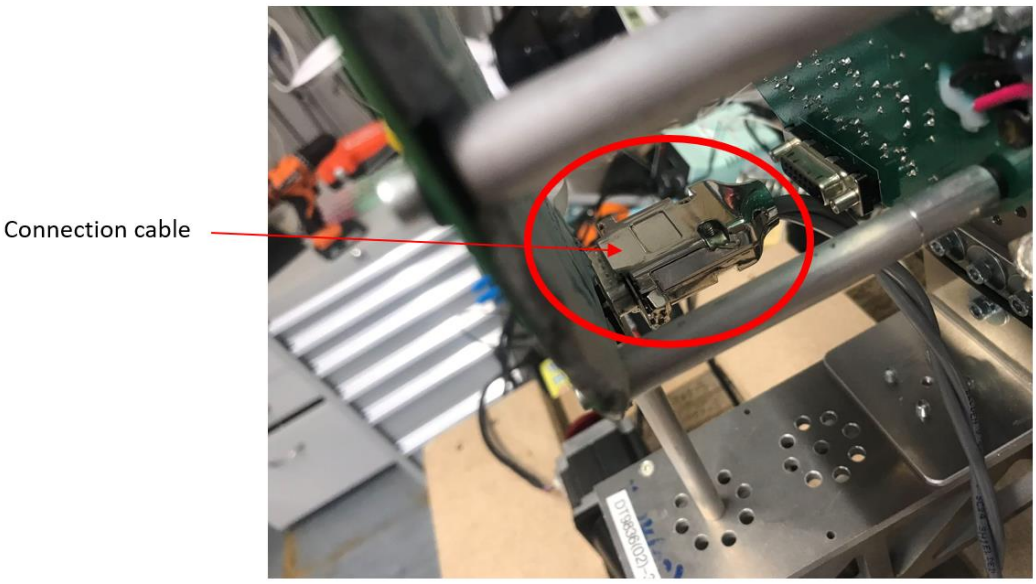

Figure 27 The transmitting signals pass through the connection cable into transducer and microphone array board.

DT9836 and DT9832A boards developed by Data Translation, now called Digilent (Digilent, 2023), have the same Analog output channels referred to in Figure 28. Table 2 shows the key features of the DT9836 and DT9832A boards.

Figure 28 DT9836 board layout with 2 DAC channels.

Table 2 Key features of Data Translation DT9836 and DT9832A analogue output and digital in/out properties

The analogue output of DT9836 and DT9832A boards		
Channels	Resolution	Speed
Up to 2	16-bit	Up to 500 kS/s/ch
Digital I/O DT9836 and DT9832A boards		
Channels	Counter/Timers	Encoder
32	2	3

2 Analog output, which was connected to the transmitting channels. The output system was assembled with 5 DT9836 boards with 10 DAC channels combined.

The transmission and reception channels across the five boards must be synchronised for the near-field focus. It was done by using a hardware trigger. The Digital I/O Connector specifications for this board are shown below:

Table 3 Digital In/Out Connector Pin Assignments

Figure 29 Digital In/Out connector (female).

Pin	Signal description	Pin	Signal description
1	Digital Input 0	20	Digital Output 0
2	Digital Input 1	21	Digital Output 1
3	Digital Input 2	22	Digital Output 2
4	Digital Input 3	23	Digital Output 3
5	Digital Input 4	24	Digital Output 4
6	Digital Input 5	25	Digital Output 5
7	Digital Input 6	26	Digital Output 6
8	Digital Input 7	27	Digital Output 7
9	Digital Input 8	28	Digital Output 8
10	Digital Input 9	29	Digital Output 9
11	Digital Input 10	30	Digital Output 10
12	Digital Input 11	31	Digital Output 11
13	Digital Input 12	32	Digital Output 12
14	Digital Input 13	33	Digital Output 13
15	Digital Input 14	34	Digital Output 14
16	Digital Input 15	35	Digital Output 15
17	Digital Ground	36	Reversed
18	Digital Ground	37	Digital Ground
19	Not Connect		

Figure 30 Digital In/Out connector(male).

From the pin assignment Table 3, digital out pin 20 has been picked for the trigger signal pin, which means choose one of the five DT9836 boards and to make it as the trigger board needs to set the MATLAB code to control the signal of pin 20 to 'RisingEdge'. Figure 29 and Figure 30 show the male/female Digital in/out connectors.

DT9836 board generates trigger signals and sends them to the external channels; then, the board can transmit and receive signals; the CT/Enc In, Analog Out, Clk/Trig Connector assignment is shown below:

Table 4 CT/Enc In, Analog Out, Clk/Trig Connector Assignments

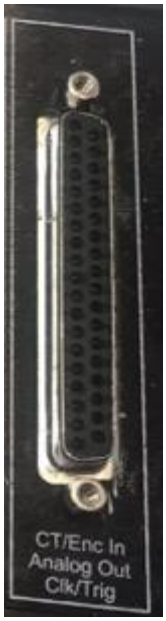

Figure 31 CT/Enc In, Analog Out, Clk/Trig Connector (female).

Pin	Signal description	Pin	Signal description
1	Analog Output 0	20	Analog Output Return 0
2	Analog Output 1	21	Analog Output Return 1
3	Analog Output 2	22	Analog Output Return 2
4	Analog Output 3	23	Analog Output Return 3
5	Digital Ground	24	Digital Ground
6	External DAC Clock	25	External DAC Trigger
7	External ADC Clock	26	External ADC Trigger
8	Counter 0 Clock	27	Digital Ground
9	Counter 0 Out	28	Counter 0 Gate
10	Counter 1 Clock	29	Digital Ground
11	Counter 1 Out	30	Counter 0 Gate
12	Quad Dec 0 A	31	Digital Ground
13	Quad 0 Index	32	Quad Dec 0 B
14	Quad Dec 1 A	33	Digital Ground
15	Quad 1 Index	34	Quad Dec 1 B
16	Quad Dec 2 A	35	Digital Ground
17	Quad 2 Index	36	Quad Dec 2 B
18	Digital Ground	37	Digital Ground
19	Not Connect		

Figure 32 CT/Enc In, Analog Out, Clk/Trig Connector (male).

The external DAC and ADC trigger, which means pin 25 and pin 26, should have the same signal simultaneously. In other words, they should be in 'RisingEdge' or 'FallingEdge' simultaneously, so they should be in series. Figure 31 and Figure 32 show female/male CT/Enc In, Analog Out, Clk/Trig Connectors.

In the original system, digital output pin 20 (Table 3) was connected to the external analogue ADC and DAC trigger pins 25 and 26 as shown in Table 4. The external DAC and ADC channels were set to start when pin 20 generated a 'Rising Edge' signal. It allowed all five boards to be synchronised.

The connection method below is used for the upgraded system with five boards to synchronise transmission and reception signals.

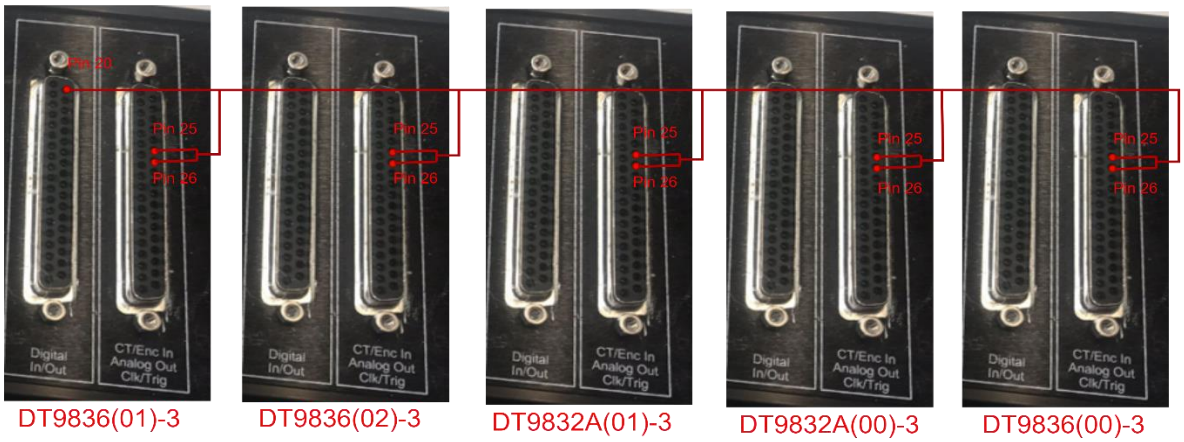

Figure 33 Upgraded system connection method.

Figure 33 shows how the trigger signal passes to the external DAC, and ADC triggers in two transmission systems.

Figure 34 shows testing performed to ensure the transmit channels were synchronised for all five boards:

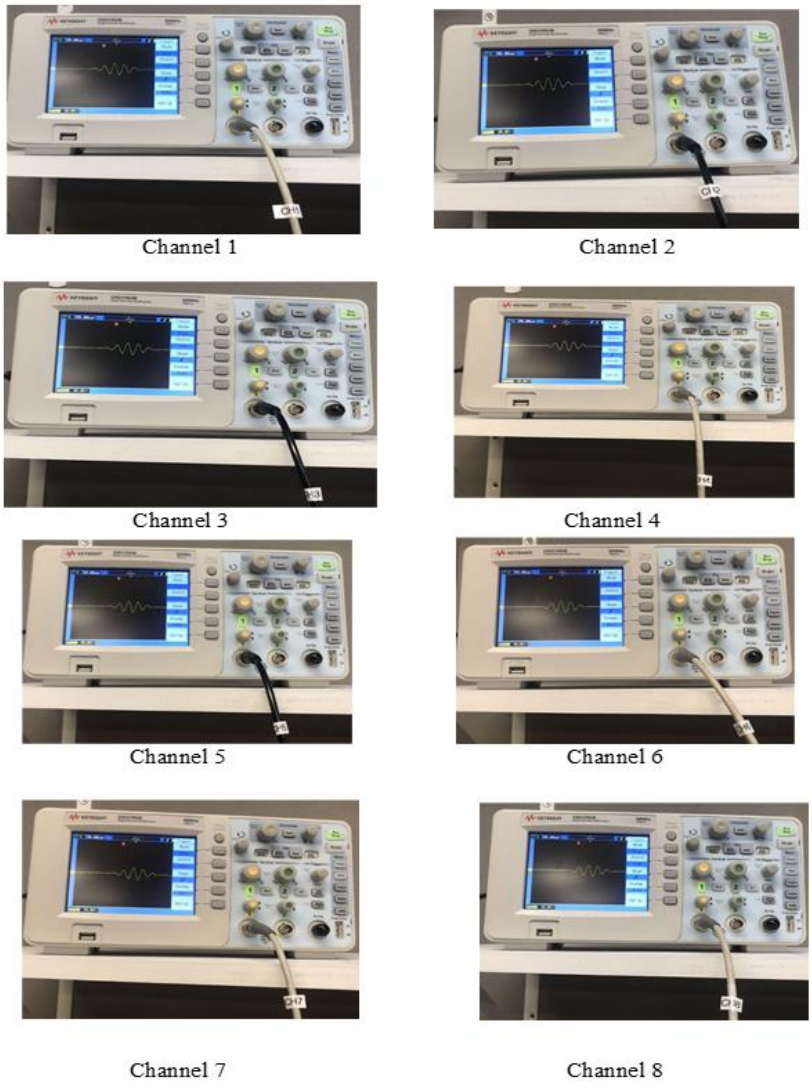

Channel 1

Channel 2

Channel 3

Channel 4

Channel 5

Channel 6

Channel 7

Channel 8

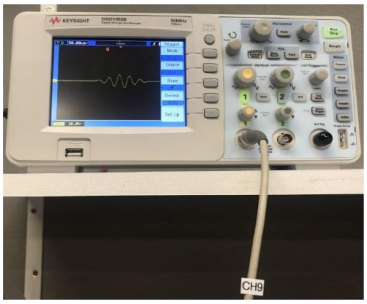

Channel 9

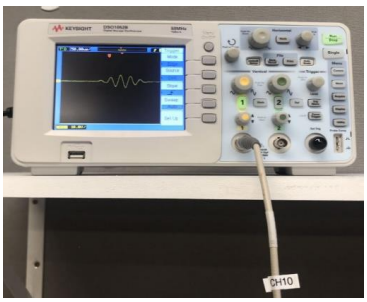

Channel 10

Figure 34 Each DAC transmitting channels working signals.

Initial testing showed that the DT9836 and DT9832A board DAC channels did have enough power to drive a single transducer channel ring for transmission. However, it was desirable to check if improved performance could be achieved by adding a power amplifier to each channel. A power amplifier system was therefore investigated. It is discussed in the following section.

3.3 Power amplifier system

The power operational amplifiers used in Legg and Bradley's original system were relatively expensive. Given the budget available, it meant that using one of these for each of the ten transmitter channels was not viable, given the budget available. A range of options were therefore investigated. The LM3886 power opamp was chosen for its relatively lower cost and characteristics. This power amplifier has been used previously for ultrasonic power amplifiers. The LM3886 is an audio power amplifier capable of delivering 68 W of continuous average power to a 4 Ω load and 38 W to an 8 Ω load (Instruments, 2013).

Rather than making a power amplifier PCB from scratch, the LM3886 DR board PCB board that was designed and produced by Neurochrome (Neurochrome, 2023) was used. Ten of these were purchased along with the required components. These were populated by hand with components and heat sinks added in our lab, giving 10 power amplifier boards.

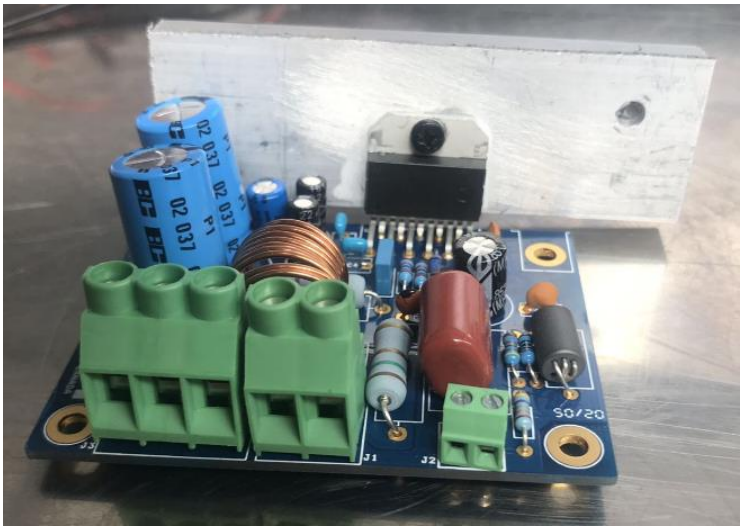

Figure 35 LM3886 DR Assembly completion.

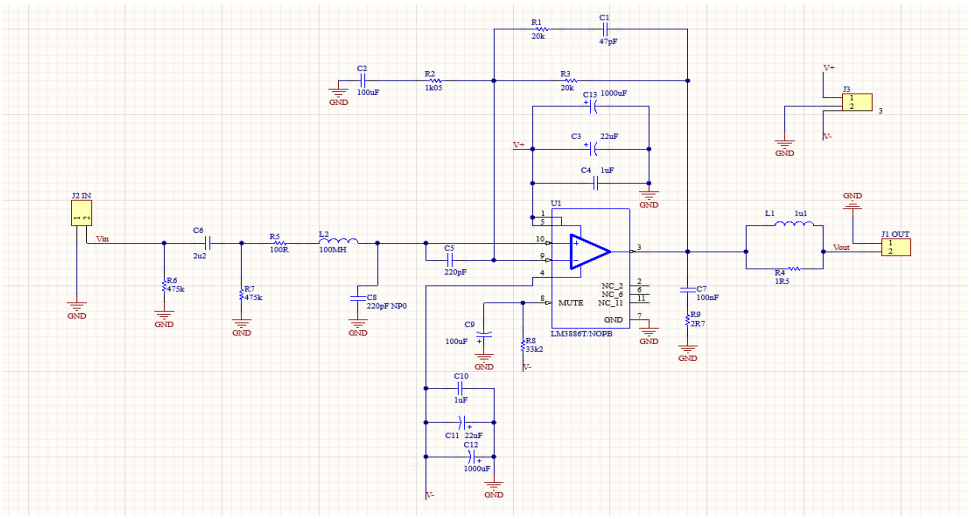

Figure 36 The schematic of LM3886 DR board.

Figure 35 shows the assembly completion of the LM3886 DR PCB board with components. Figure 36 shows the schematic of the LM3886 DR PCB board.

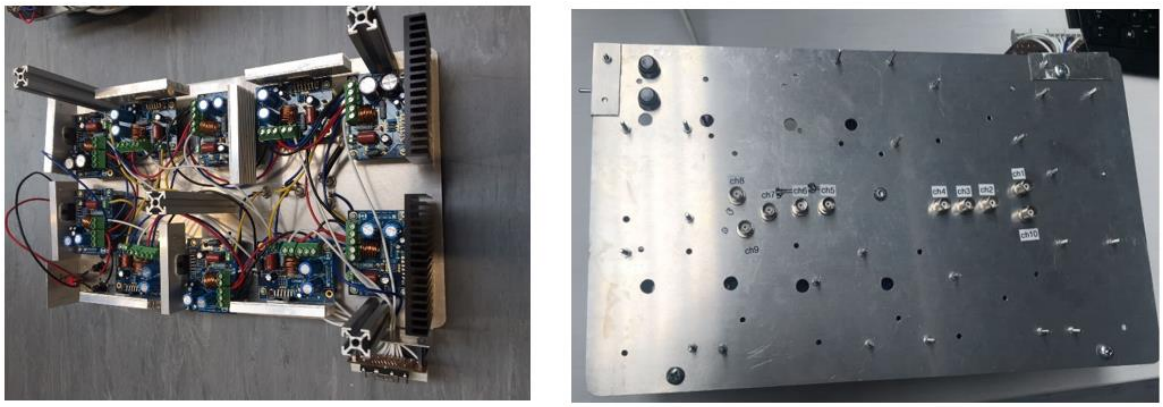

(a) Front side of the amplifier system (b) Back side of the amplifier system

Figure 37 The amplifier system.

Figure 37(a) shows the amplifier system consists of 10 LM3886 DR amplifiers. They are fixed to and insulated from the metal plate. The power connection is in series. Each amplifier has separate input and output channels. Figure 37(b) shows that it has 10 separate BNC inputs on the metal plate that can receive the signals from the DT9836 board. The amplified transmission signal can be passed to the transmitting board and drive the transducers to transmit the amplified signals through the connection between the Output Connector and connection Cable.

3.3.1 Testing amplifiers

The amplifiers were tested to ensure they worked properly at the rated voltage, see Figure 38.

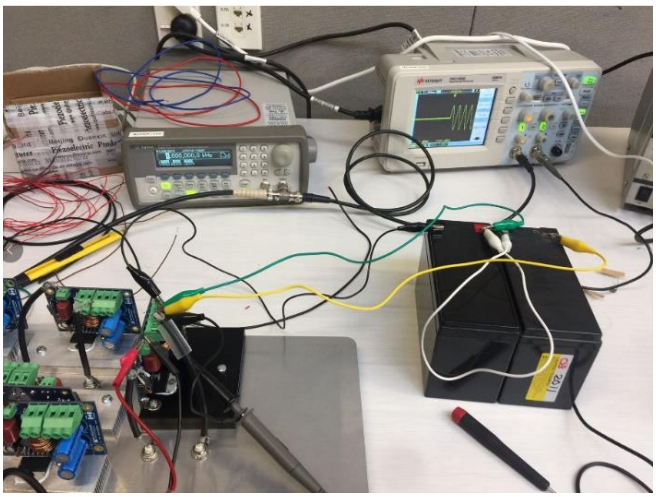

Figure 38 Individual amplifier testing shows they work normal under rated voltage.

The maximum supply voltage is ±35 V, and the minimum is ±10 V. The operational voltage used here was around ±25 V. The amplifier works appropriately at the rated voltage, which also verifies that there are no errors during assembly, see Figure 38. However, during the assembly test with the oscilloscope, it was found that there was more noise on the output signal compared with the input signal applied directly from the DAC, see Figure 39.

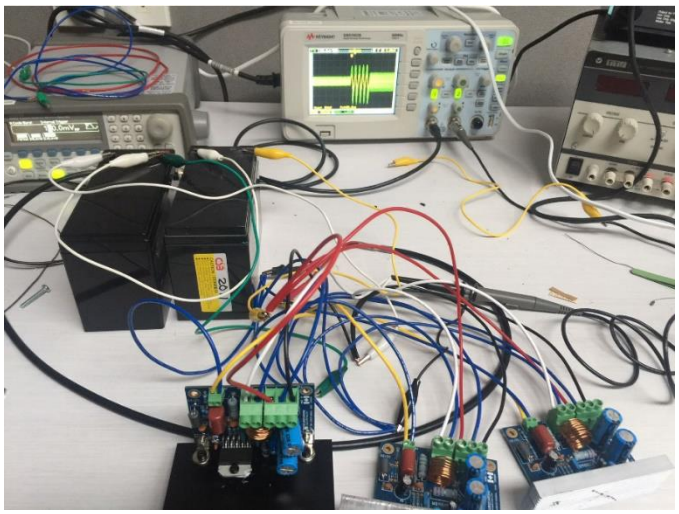

Figure 39 Noise occurs when multiple testing more than two amplifiers.

After analysis, it is suspected that it results from excessive gain. It is necessary to lower the gain to avoid the system's noise in further work to be consistent with the original system. However, at this stage, it was decided, due to time constraints, not to use the power amplifiers as the DT9836 and DT9832A boards could be used to drive the transducer channels with lower noise levels.

3.4 Angular measurement system

The measurements were needed at various angles to study the transmit and receive beam patterns with far-field and near-field focusing. It was achieved by mounting the transmitting and reception array PCB board onto a turntable system. The turntable used was the CNC Rotary Indexer (CRI), which was developed by Sherline (Sherline, 2023) for milling machines and can rotate precisely in an angular manner and can be manipulated through MATLAB code and digital outputs of the DT9836 board.

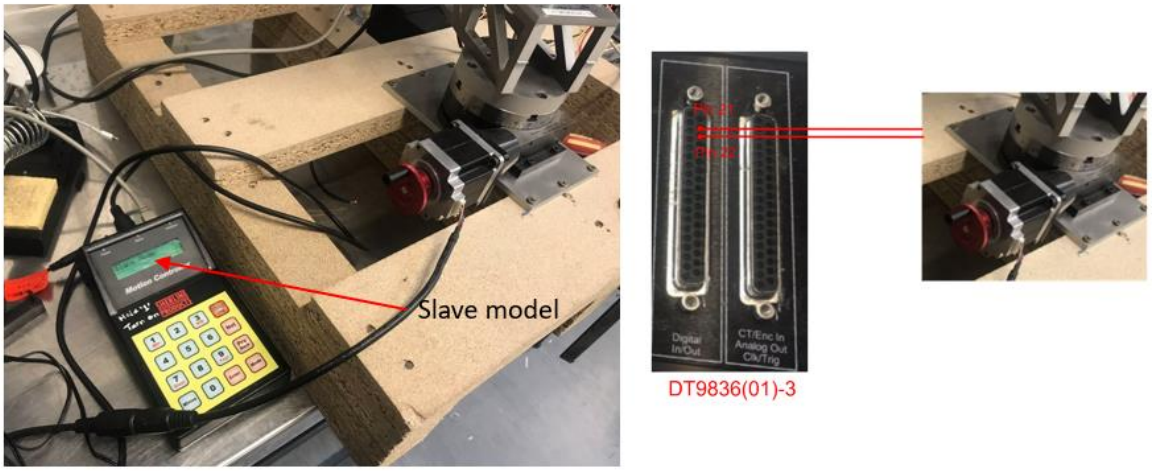

(a) CNC Rotary Indexer including keypad and rotary table

(b)Pin 21 and 22 were chosen to generate driven signals to CNC Rotary Indexer

Figure 40 CNC Rotary Indexer including keypad and rotary table.

Figure 40 shows that the CRI is divided into two modes of operation: ‘manual’ and ‘slave’. Slave mode was used by pressing the '1' and power buttons together. Slave mode requires connecting the CRI to the DT9836 board and using MATLAB code on the computer to operate.

The slave mode connection should be clarified. Table 3 shows that the digital output pins 21 and 22 have been picked as the CRI control signals. Outputting a high and low digital signal on digital output 21 caused the turntable to move a step ($1/80^{th}$ of a degree). Digital output 22 was used to control the direction of movement. When the DT9836 board generates signals, the CRI moves and stops under slave mode. It allows the transmitting and reception system to accurately simulate the rotational scanning situation. When the program runs, the entire system scans the target following the CNC Rotary Indexer and the collected data is stored in the DT9836 board.

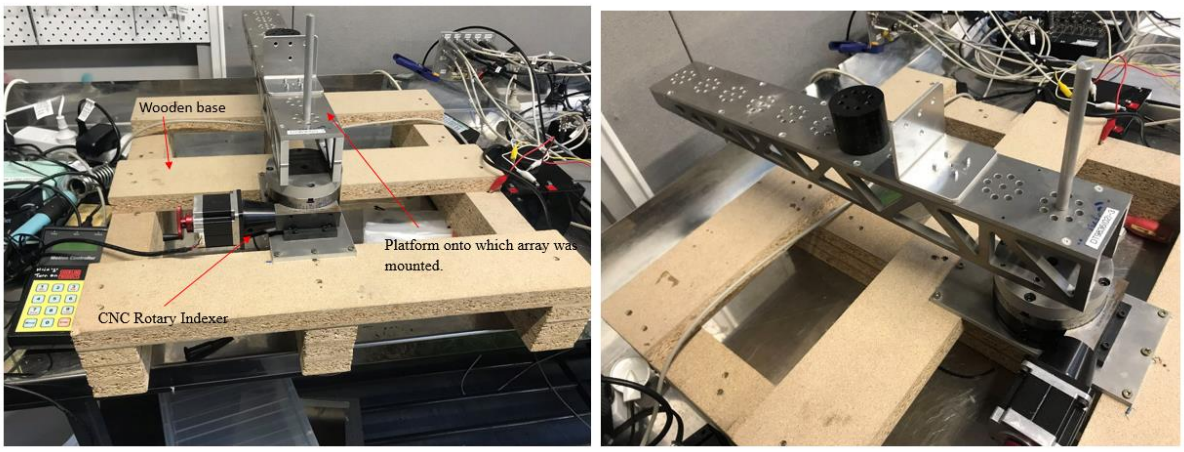

Figure 41 CNC Rotary Indexer and wooden base.

Figure 41 shows that the CNC Rotary Indexer was placed in the middle of a wooden base. An aluminium arm was then attached to the top of the CNC Rotary Indexer. This arm was used to position the ultrasonic array such that the front of the array was at the centre of rotation. The

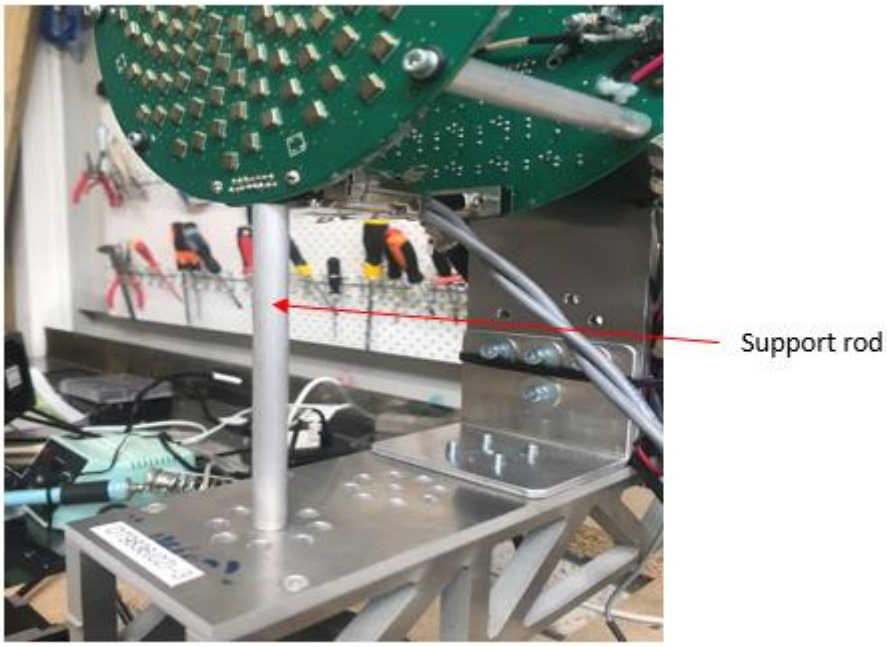

Figure 42 A support rod was placed under the array board.

support rod was positioned under the array PCB board to prevent sagging, as referred to in Figure 42.

Figure 43 A plastic cube stick on a metal rod.

Figure 43 shows a flat plastic cube fixed onto a metal rod as the target to receive the signals and reflect echoes to the microphones.

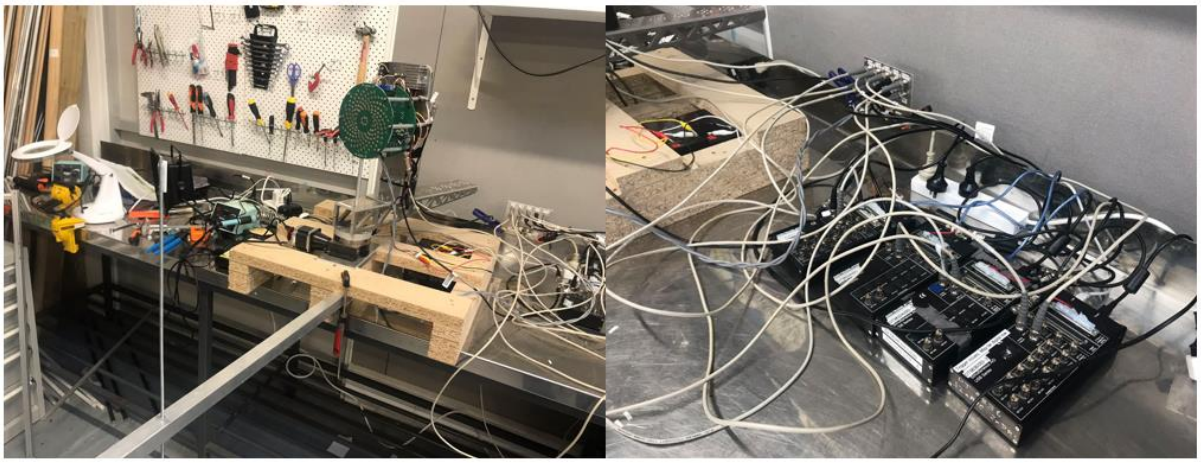

Figure 44. Final layout. Including five DT9836 and DT9832A boards.

Figure 44 illustrates the final layout of the test, including the transmission and reception system.

3.5 Measurement Process

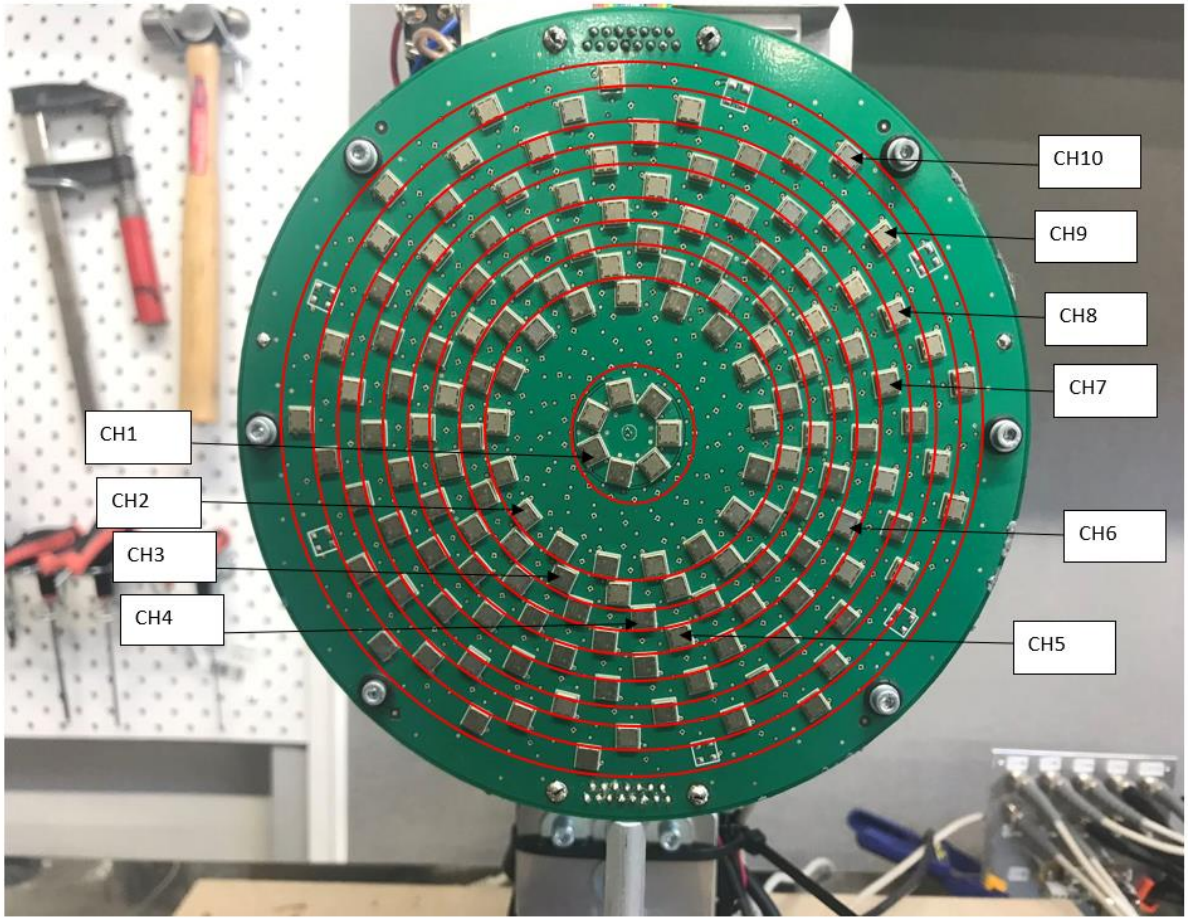

Figure 45 Transducer and microphone array PCB board. Transmit transducer rings are shown.

Figure 45 shows 10 transmitting rings that transmit ultrasonic waves controlled by DT9836 boards. Under the control of MATLAB code, the DACs channels of the five DT9836 and DT9832A boards generate 10 independent channels of sine wave signals applied to the 10 rings of transducers. The transmit signal is 5 cycles of a sine wave with an amplitude of up to 7 Vpp. A transmit sampling rate of 500 kHz and a resolution of 16 bits was used. The transmit array focuses on the far field if the same signal is applied to each channel. However, delays may be added to each channel to allow the focusing of the transmit signal in the near field using beamforming techniques. (Note that during the experiments, it was found that transmit rings 2 and 3 did not transmit sound. Due to time constraints, the exact course of this could not be identified. However, it may have been due to an internal electrical short on these transmit channels or damage to a track.)

The transmitted (TX) acoustic signal is reflected off an object and received (RX) by the microphones in the array. The 12 summon preamplifiers combine the signal from each microphone ring, resulting in 12 amplified/filtered analogue microphone signals. These are then sampled by the 12 ADC channels using a sampling rate of 225 kHz with a resolution of 16 bits. If the 12 ADC data channels are summed, this results in a single channel of microphone data focused in the far-field. However, beamforming may focus the receiver array at a point in the near field. It is done by delaying each channel before summing the data. Cross-correlation with the transmit signal may be used to improve depth resolution.

Experiments were first conducted with the turn table system to obtain the beam pattern of the array using different combinations of near-field and far-field beamforming for transmission and reception. Following this, experiments were performed on pasture samples in the lab. These measurements are presented in chapters 4 and 5, respectively.

4. Beam pattern measurements

4.1 Experiment design

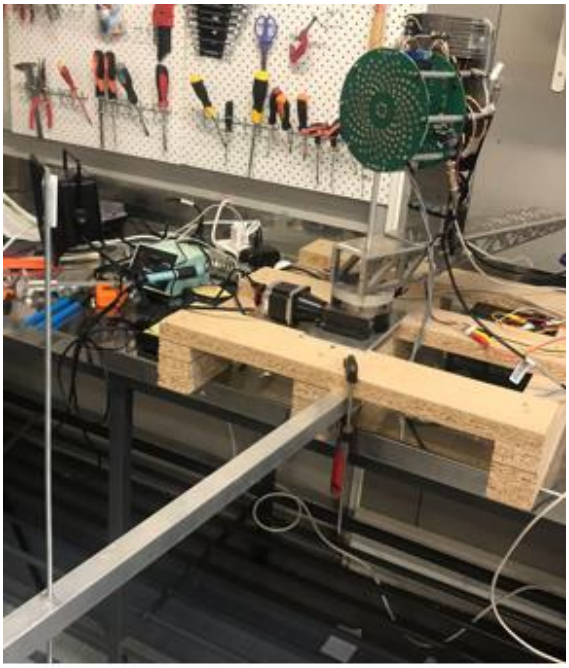

Figure 46 The transducer array and target.

Experiments were carried out to evaluate the array's transmitting and receiving beam patterns using different combinations of near-field and far-field beamforming for transmitting and receiving. The array was mounted onto the CNC turntable, and a 600 mm long and 6 mm diameter rod (acting as an acoustic reflector) was positioned in front at either 300mm or 700mm from the array, as shown in Figure 46. The turntable was incrementally moved in steps of 0.2 degrees while the rod remained stationary. Measurements were made at each position of the turntable. The transmitting signal was a 5-cycle sine wave pulse with a central frequency of either 20 or 60 kHz, discussed in section 1.3.1 Transducer ringing effects., with far-field or near-field transmission beamforming. These frequencies were chosen to reduce transducer ringing, which would reduce depth resolution relative to that for the resonance frequency of 40 kHz. After each experiment, the received signals are processed using far-field and near-field receive beamforming.

4.2 Experiment data for rod at 700mm

The array diameter is 85mm. Therefore, 700 mm is close to being in the far-field of the array. Hence, focusing on infinity (referred to here as far-field focusing) should not have too detrimental an effect compared to focusing on the correct distance of 700 mm (referred to here as near-field focusing).

4.2.1 The experiment data of 20 kHz 700mm with TX near

Table 5 Key parameters of the experiment

Experiment serial number	Target distance(mm)	Transmitting signal frequency(kHz)	Transmitting signal type (Pulse)	Transmitting signal beamforming	Receiving signal beamforming
1.1	700	20	5-cycle sine waves	TX near	RX near
	700	20	5-cycle sine waves	TX near	RX far

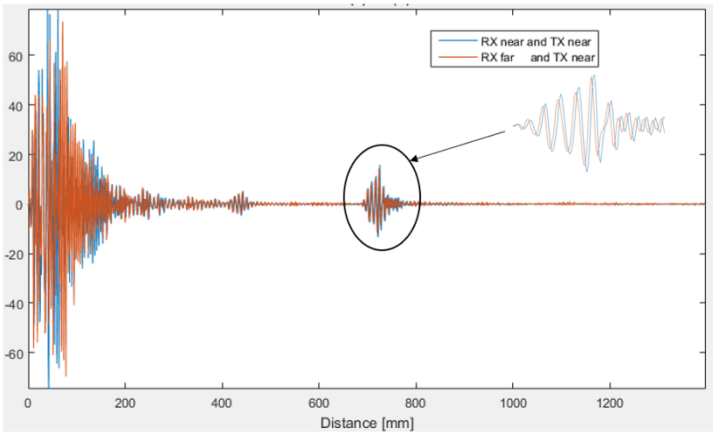

Figure 47 Example of raw echo signal for array facing the rod, located at 700 mm from array. Red corresponds to near-field transmitter beamforming and far-field receiver beamforming. Blue stand for both near-field transmitter and receiver beamforming. (20 kHz 700mm)

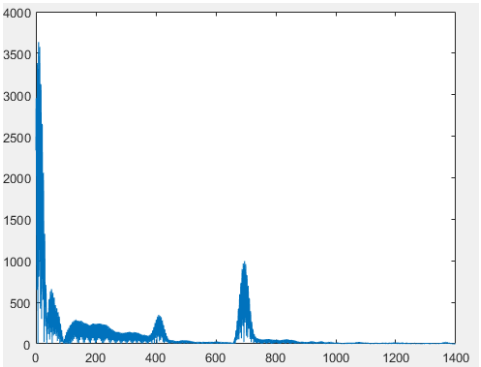

Figure 48 Figure shows the cross-correlation signals when the array was facing the rod located at 700 mm.

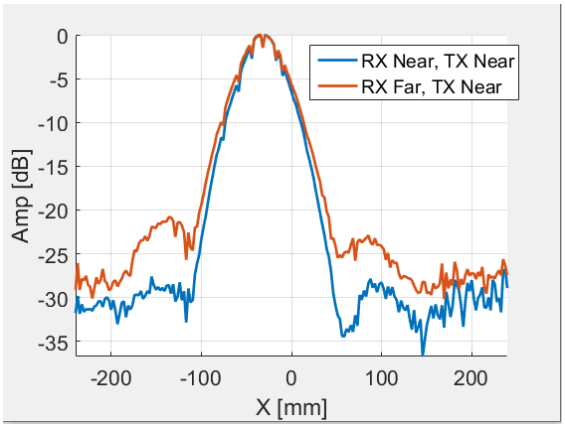

(a)The distance beampattern.

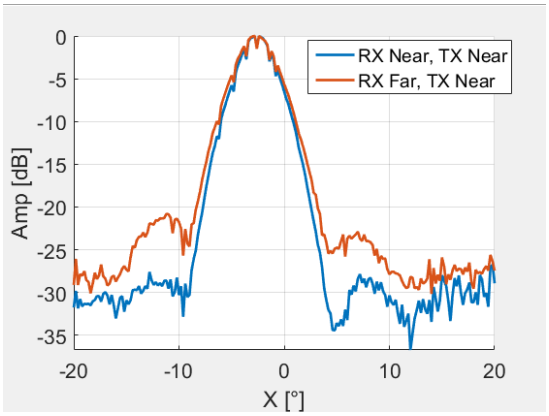

(b)The angle beampattern.

Figure 49 Comparison of receiver (RX) near and far field focusing for distance (left) and angle (right) beampatterns when the transmit(TX) signal is focusing near field.

Table 5 shows the key parameters of the experiment. Figure 47 shows the raw echo signal when the array faces the rod. Figure 48 shows the cross-correlation signals when the array faces the rod.

From Figure 49, when the target is 700mm away from the transmitting board, and one focuses on the near field for the transmitting signals, the blue line (RX and TX near field) has a narrower beamwidth below -3dB. That means below -3dB, reception signals focusing near field and transmitting signals focusing near field (RX near and TX near) can get slightly narrower beamwidth than reception signals far field and transmitting near field (RX far and TX near) focusing.

4.2.2 The experiment data of 20kHz 700mm with TX far

Table 6 Key features of the experiment

Experiment serial number	Target distance(mm)	Transmitting signal frequency(kHz)	Transmitting signal type (Pulse)	Transmitting signal beamforming	Receiving signal beamforming
1.2	700	20	5-cycle sine waves	TX far	RX near
	700	20	5-cycle sine waves	TX far	RX far

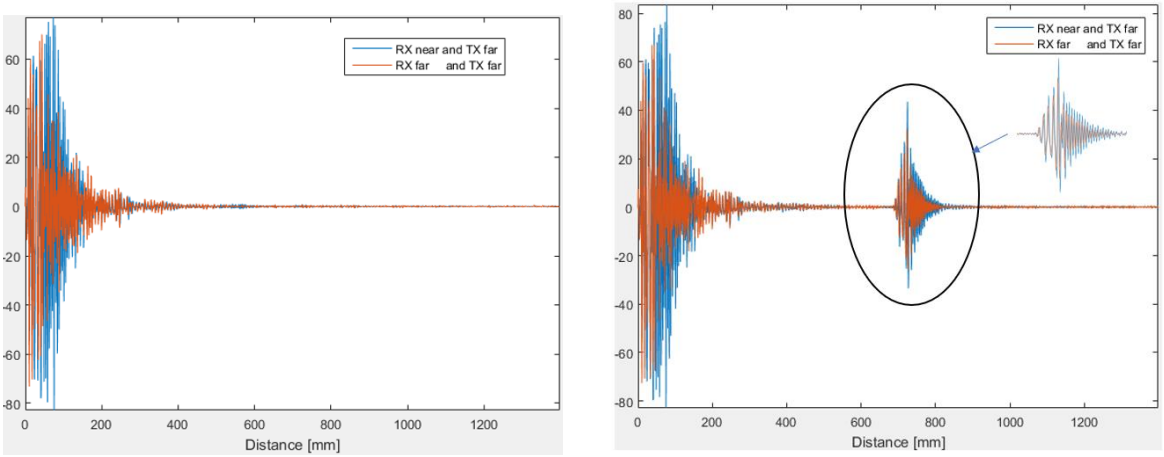

(a) The raw signal when array turned 20 degrees away from the rod.

(b) The raw signal when array faced the rod.

Figure 51 Example raw signal when near and far field receiver (RX) focusing with transmission (TX) focusing on the far field. The left figure shows the array turned 20 degrees away from the rod. The right-side figure shows the array facing the rod.(20 kHz 700mm)

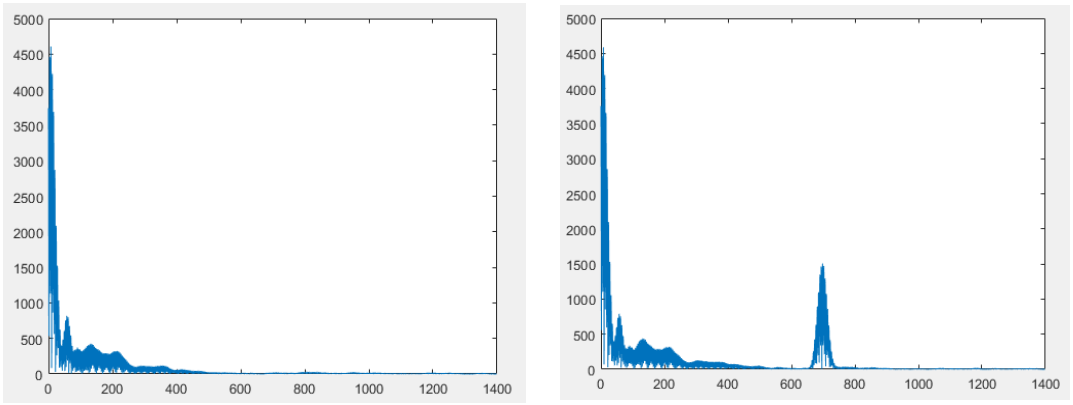

(a) The cross-correlation signal when array turned 20 degrees away from the rod.

(b) The cross-correlation signal when array faced the rod.

Figure 50 The left figure shows the cross-correlation signal when the array is pointed away from the rod target. The right-side figure shows the cross-correlation signal when transmitting board is facing the target.

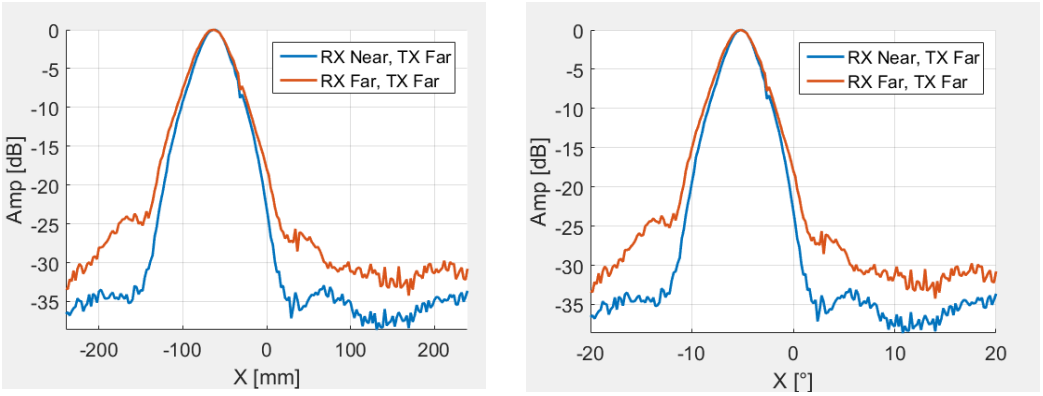

(a) The distance beampattern.

(b) The angle beampattern.

Figure 52 Comparison of receiver (RX) near and far field focusing for distance (left) and angle (right) beampatterns when the transmit signal is focusing far field.

Comparing the graphics under two conditions gives the figure below:

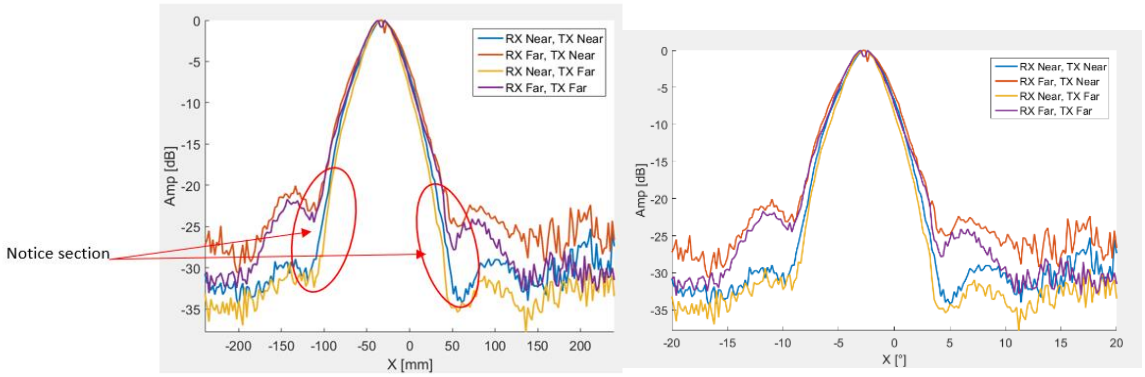

(a) The distance beampattern comparison.

(b) The angle beampattern comparison.

Figure 53 Combination pictures of the different combinations of focusing of reception (RX) and transmission (TX) at20 kHz 700mm. (a)(b) stand for comparing in millimetre and degree.

Table 6 shows the key parameters of the experiment. Figure 51 shows the raw signals when the transmitting array focuses far field. Figure 50 shows the cross-correlation signals from the raw signals. Figure 52 shows the comparison of the receiver near and far field focusing for distance and angle beampatterns when transmitting signal is focusing far field.

Figure 53 shows that near-field beamforming for reception has the best results. Transmit focusing here has minimal effect.

4.3 The experiment data of 60kHz 700mm

4.3.1 The experiment data of 60kHz 700mm with TX near

Table 7 Key features of the experiment

Experiment serial number	Target distance(mm)	Transmitting signal frequency(kHz)	Transmitting signal type (Pulse)	Transmitting signal beamforming	Receiving signal beamforming
1.3	700	60	5-cycle sine waves	TX near	RX near
	700	60	5-cycle sine waves	TX near	RX far

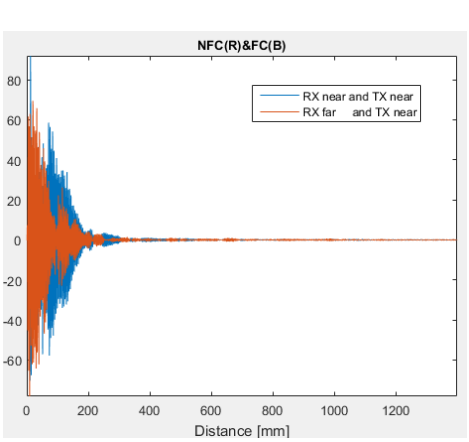

(a) The raw signal when array turned 20 degrees away from the rod.

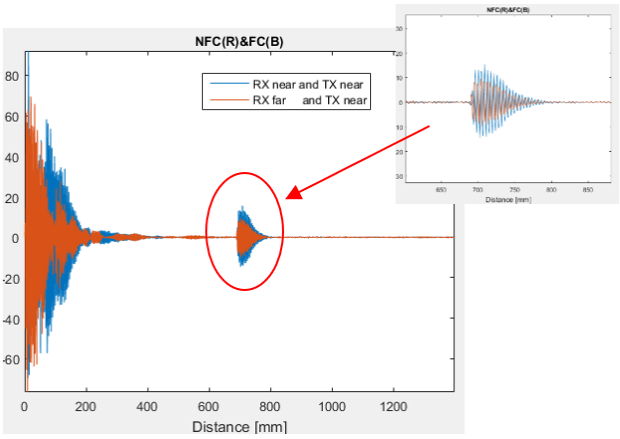

(b) The raw signal when array faced the rod.

Figure 54 Example raw signal when near and far field receiver (RX) focusing with transmission (TX) focusing on the near field. The left figure shows the array turned 20 degrees away from the rod. The right-side figure shows the array facing the rod. (60 kHz 700mm)

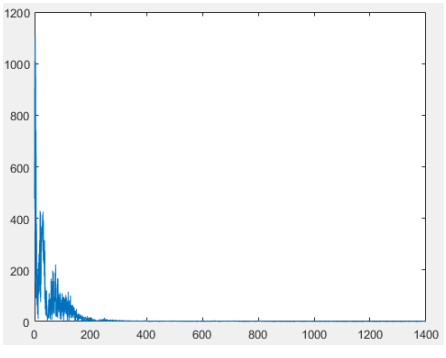

(a) The cross-correlation signal when array turned 20 degrees away from the rod.

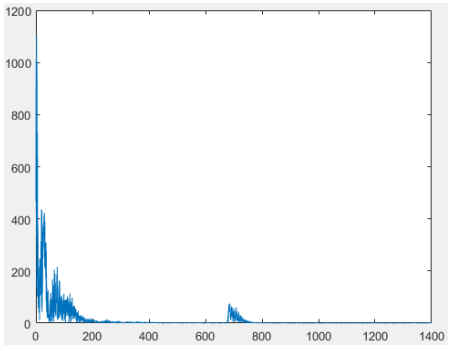

(b) The cross-correlation signal when array faced the rod.

Figure 55 The left figure shows the cross-correlation signal when the array is pointed away from the rod target. The right-side figure shows the cross-correlation signal when transmitting board is facing the target.

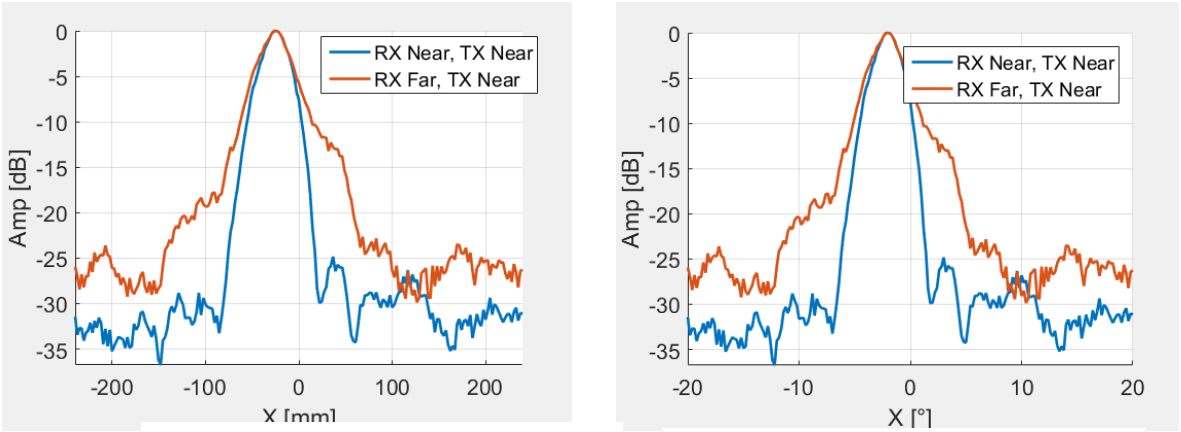

(a) The distance beampattern.

(b) The angle beampattern.

Figure 56 Comparison of receiver (RX) near and far field focusing for distance (left) and angle (right) beampatterns when the transmit signal is focusing near field.

Table 7 shows the key parameters of the experiment. Figure 54 shows the raw signal when near and far field receiver (RX) focusing with transmission (TX) focusing on the near field. Figure 55 shows the cross-correlation signal from the raw signal.

Figure 56 shows when the target is 700mm away from the transmitting board at 60 kHz and focusing the array in the near field, the blue line (RX and TX near field) has a narrower beamwidth below -3dB. That means below -3dB, reception signals focusing near field and transmitting signals focusing near field (RX near and TX near) can get slightly narrower beamwidth than reception signals far field and transmitting near field (RX far and TX near) focusing.

4.3.2 The experiment data of 60kHz 700mm with TX far

Table 8 Key parameters of the experiment

Experiment serial number	Target distance(mm)	Transmitting signal frequency(kHz)	Transmitting signal type	Transmitting signal beamforming	Receiving signal beamforming
1.4	700	60	5-cycle sine waves	TX far	RX near
	700	60	5-cycle sine waves	TX far	RX far

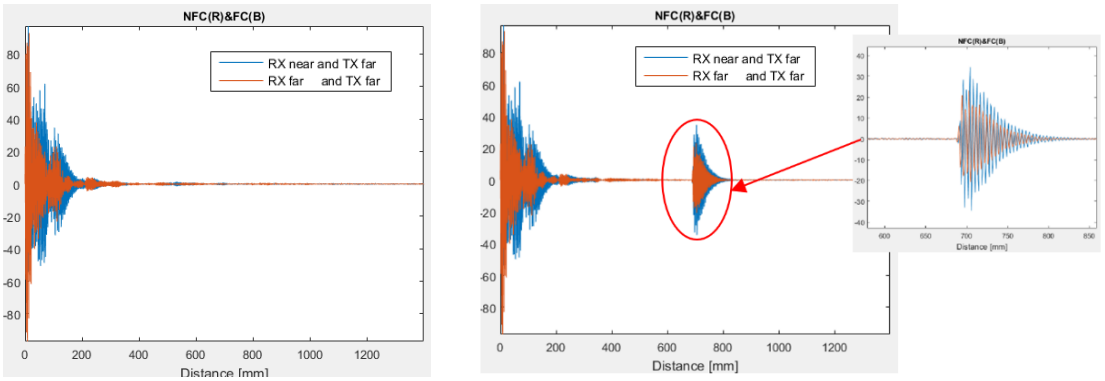

(a) The raw signal when array turned 20 degrees away from the rod.

(b) The raw signal when array faced the rod.

Figure 57 Example raw signal when near and far field receiver (RX) focusing with transmission (TX) focusing on the far field. The left figure shows the array turned 20 degrees away from the rod. The right-side figure shows the array facing the rod. (60 kHz 700mm)

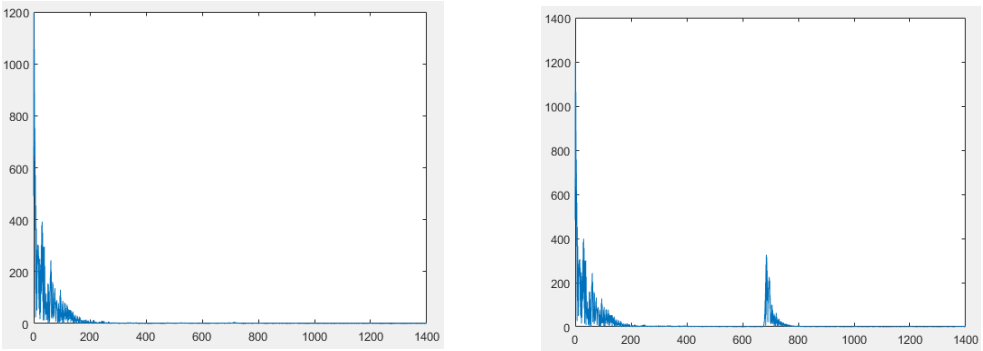

(a) The cross-correlation signal when array turned 20 degrees away from the rod.

(b) The cross-correlation signal when array faced the rod.

Figure 58 The left figure shows the cross-correlation signal when the array is pointed away from the rod target. The right-side figure shows the cross-correlation signal when transmitting board is facing the target.

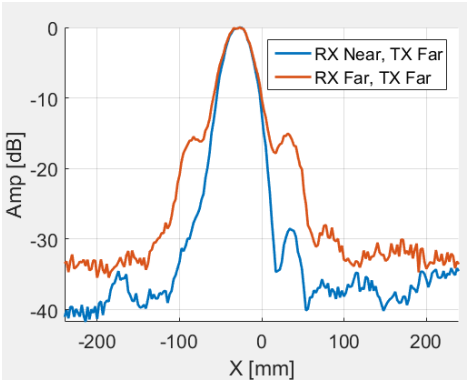

(a) The distance beampattern.

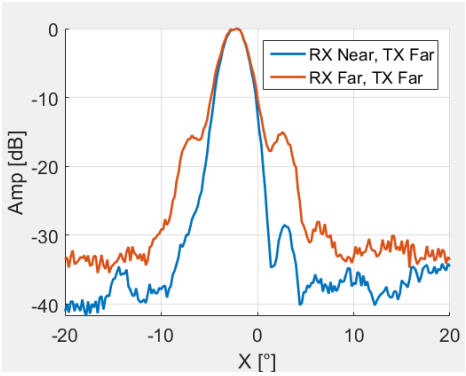

(b) The angle beampattern.

Figure 59 Comparison of receiver (RX) near and far field focusing for distance (left) and angle (right) beampatterns when the transmit signal is focusing far field.

Table 8 shows the key parameters of the experiment. Figure 57 shows the raw signal when transmission focuses far field. Figure 58 shows the cross-correlation signal from the raw signal. Figure 59 shows when the target is 700mm away from the transmitting board, and the transmitting signals TX uses far-field focusing, the blue line is narrower than the red line below -3dB. That means below -3dB, receiving signals focused near field and transmitting signals focused far field can get more focusing results than receiving signals focused far field and transmitting signals focused far field.

Comparing the graphics under two conditions gives the figure below:

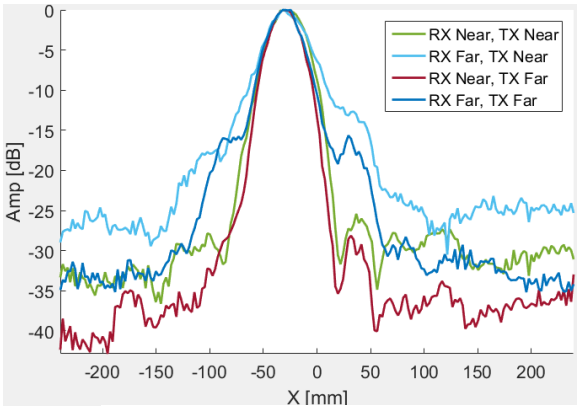

(a) The distance beampattern.

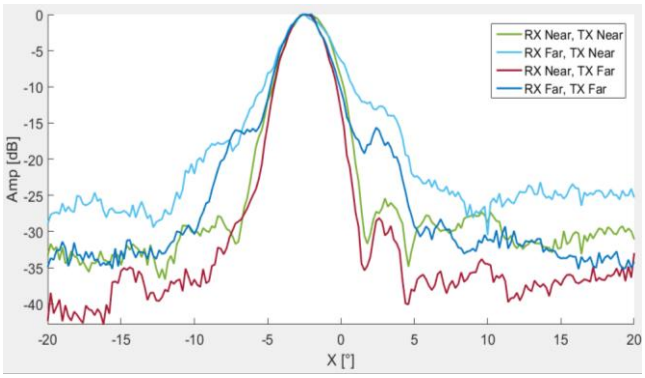

(b) The angle beampattern.

Figure 60 Combination waveform of the different combination of reception (RX) and transmission (TX) focusing near and Tx far for 60kHz with the reflector located at 700mm from the array.

Figure 60 shows when it is at -3dB and below, whether transmitting signals focus near or far field, the curves coincide, and the difference is minimal. Below -3dB, it can be seen that the green and red lines converge more closely than the other two lines. Focusing reception and transmission array in the near field is comparable with focusing reception array near field and transmission far field. However, the latter gives slightly better results below about -30 dB.

4.4 The experiment data of 20kHz 300mm

4.4.1 The experiment data of 20kHz 300mm with TX near

Table 9 Key parameters of the experiment

Experiment serial number	Target distance(mm)	Transmitting signal frequency(kHz)	Transmitting signal type	Transmitting signal beamforming	Receiving signal beamforming
1.5	300	20	5-cycle sine waves	TX near	RX near
	300	20	5-cycle sine waves	TX near	RX far

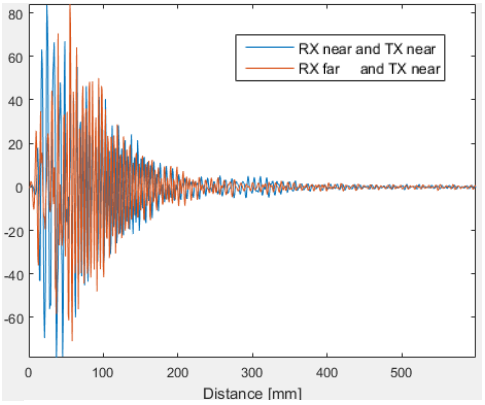

(a) The raw signal when array turned 20 degrees away from the rod.

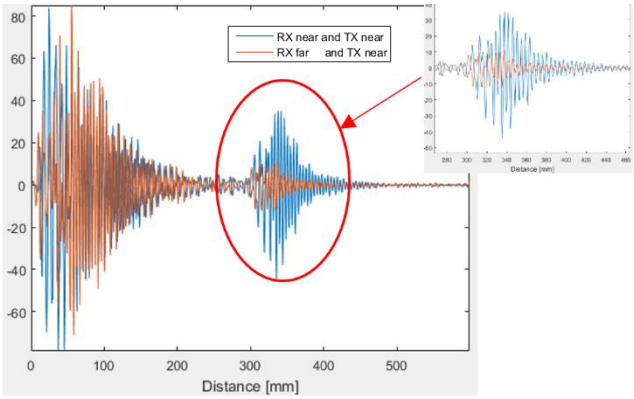

(b) The raw signal when array faced the rod.

Figure 61 Example raw signal when near and far field receiver (RX) focusing with transmission (TX) focusing on the near field. The left figure shows the array turned 20 degrees away from the rod. The right-side figure shows the array facing the rod. (20 kHz 300mm)

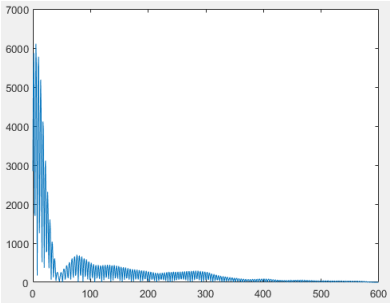

(a) The cross-correlation signal when array turned 20 degrees away from the rod.

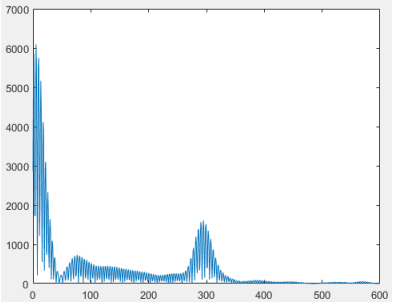

(b) The cross-correlation signal when array faced the rod.

Figure 62 The left figure shows the cross-correlation signal when the array is pointed away from the rod target. The right-side figure shows the cross-correlation signal when transmitting board is facing the target.

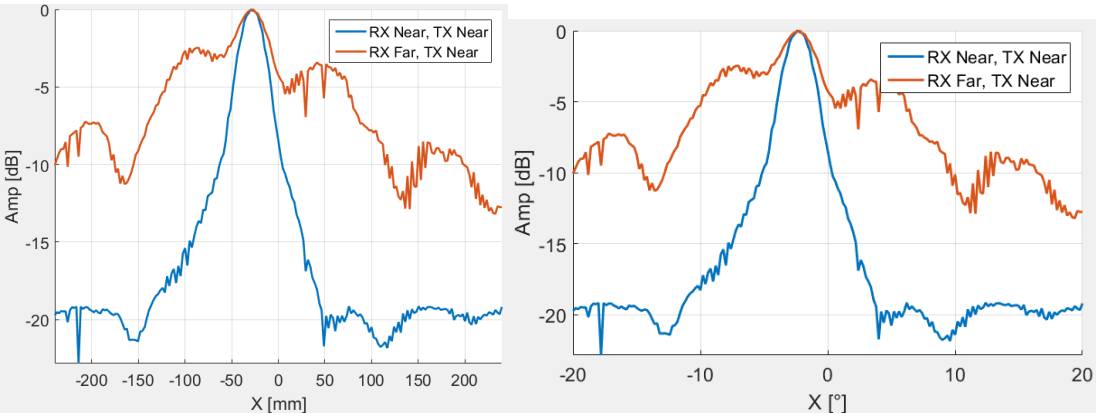

(a) The distance beampattern. (b) The angle beampattern.

Figure 63 Comparison of receiver (RX) near and far field focusing for distance (left) and angle (right) beampatterns when the transmit signal is focusing near field.

Table 9 shows the key parameters of the experiment. Figure 61 shows the raw signal when near and far field receiver (RX) focusing with transmission (TX) focusing on the near field. Figure 62 shows the cross-correlation signal from the raw signal.

Figure 63 shows when the target is 300mm from the transmitting board at 20 kHz, and the transmitting signal is TX near. The blue line is narrower than the red line below -3dB. That means below -3dB, focusing the array in the near field can get more focusing results than focusing the transmitting array in the near field and receiving array in the far field.

4.4.2 The experiment data of 20kHz 300mm with TX far

Table 10 Key parameters of the experiment

Experiment serial number	Target distance(mm)	Transmitting signal frequency(kHz)	Transmitting signal type	Transmitting signal beamforming	Receiving signal beamforming
1.6	300	20	5-cycle sine waves	TX far	RX near
	300	20	5-cycle sine waves	TX far	RX far

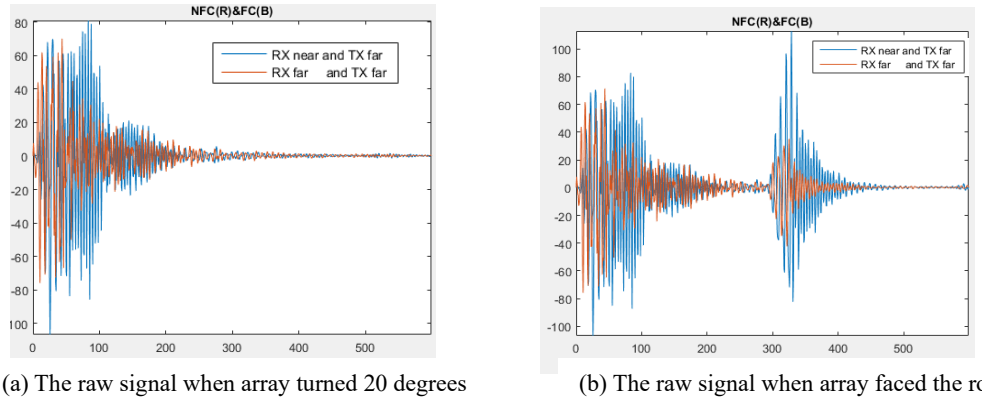

(a) The raw signal when array turned 20 degrees away from the rod.

(b) The raw signal when array faced the rod.

Figure 64 Example raw signal when near and far field receiver (RX) focusing with transmission (TX) focusing on the far field. The left figure shows the array turned 20 degrees away from the rod. The right-side figure shows the array facing the rod. (20 kHz 300mm)

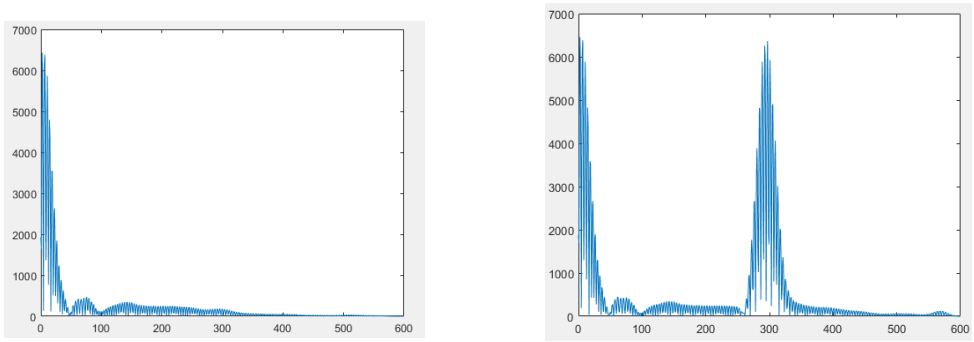

(a) The cross-correlation signal when array turned 20 degrees away from the rod.

(b) The cross-correlation signal when array faced the rod.

Figure 65 The left figure shows the cross-correlation signal when the array is pointed away from the rod target. The right-side figure shows the cross-correlation signal when transmitting board is facing the target.

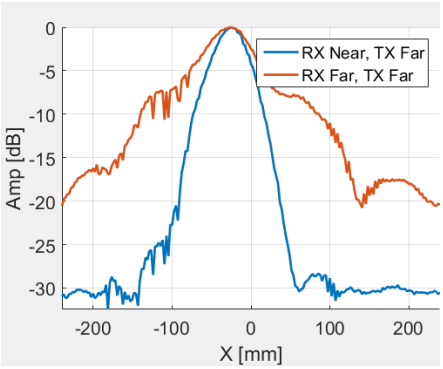

(a) The distance beampattern.

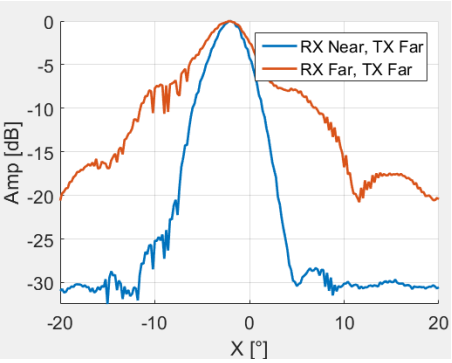

(b) The angle beampattern.

Figure 66 Comparison of receiver (RX) near and far field focusing for distance (left) and angle (right) beampatterns when the transmit signal is focusing far field.

Table 10 shows the key parameters of the experiment. Figure 64 shows the raw signal when near and far field receiver (RX) focusing with transmission (TX) focusing on the far field. Figure 65 shows the cross-correlation signal from the raw signal. Figure 66 shows when the target is 300mm from the transmitting board and the transmitting signals are TX far. The blue line is narrower than the red line below -3dB. That means below -3dB, reception and transmission focus near field can get more focusing results than reception and transmission focus far field.

Comparing the graphics under two conditions, it can get the figure below:

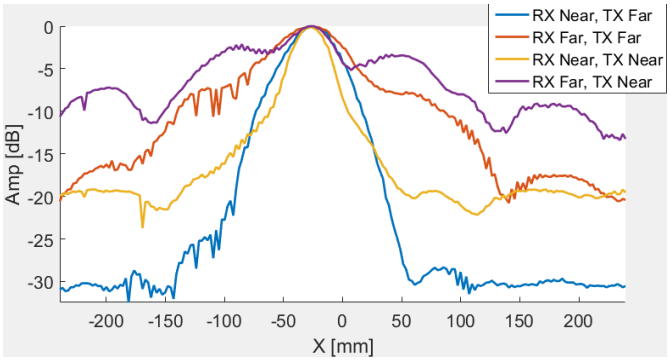

(a) The distance beampattern.

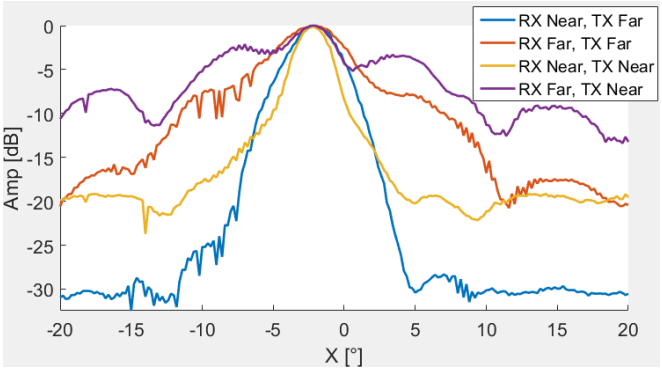

(b) The angle beampattern.

Figure 67 Comparison of beampatterns for different focusing of receiver (RX) and transmitter for distance and angle at 20 kHz 300mm.

Figure 67 shows that between approximately -3dB and -13dB, the yellow curve, which focuses the array in the near field, is the narrowest, meaning it has the most accurate result. The blue curve is narrower than the yellow curve when the amplitude is below -13dB. However, for two conditions, focusing the array in the near field and focusing reception in the near field but transmission in the far field, they both have narrower curves than the other two.

4.5 The experiment data of 60kHz 300mm

4.5.1 The experiment data of 60kHz 300mm with TX near

Table 11 Key parameters of the experiment

Experiment serial number	Target distance(mm)	Transmitting signal frequency(kHz)	Transmitting signal type	Transmitting signal beamforming	Receiving signal beamforming
1.7	300	60	5-cycle sine waves	TX near	RX near
	300	60	5-cycle sine waves	TX near	RX far

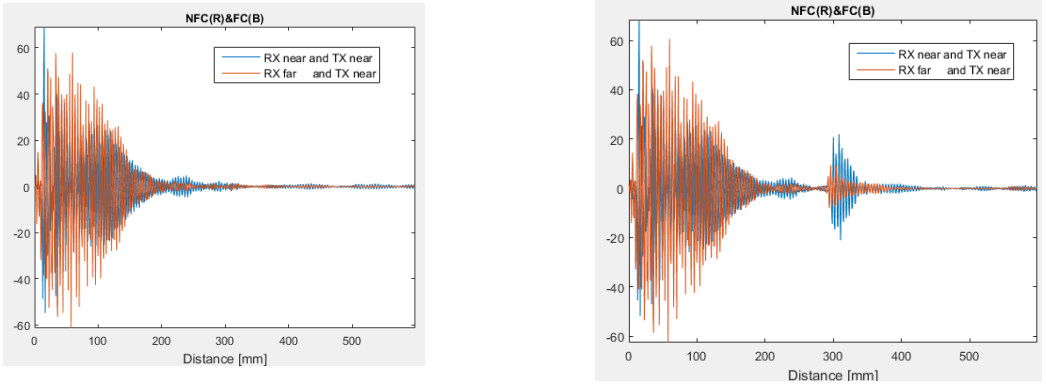

(a) The raw signal when array turned 20 degrees away from the rod.

(b) The raw signal when array faced the rod.

Figure 68 Example raw signal when near and far field receiver (RX) focusing with transmission (TX) focusing on the near field. The left figure shows the array turned 20 degrees away from the rod. The right-side figure shows the array facing the rod. (60 kHz 300mm)

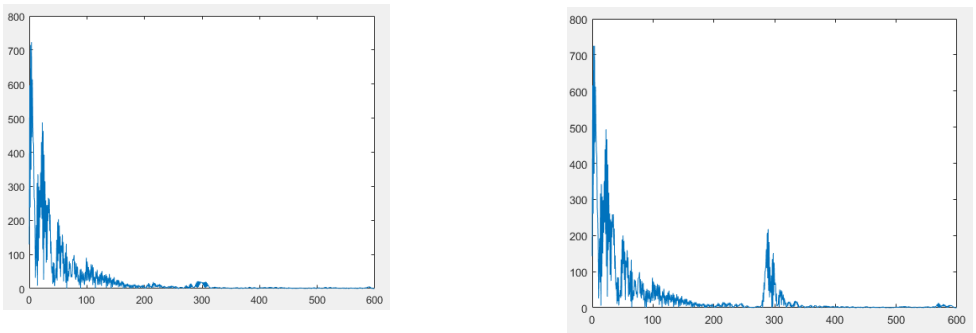

(a) The cross-correlation signal when array turned 20 degrees away from the rod.

(b) The cross-correlation signal when array faced the rod.

Figure 69 The left figure shows the cross-correlation signal when the array is pointed away (20 degrees) from the rod target. The right-side figure shows the cross-correlation signal when transmitting board is facing the target.

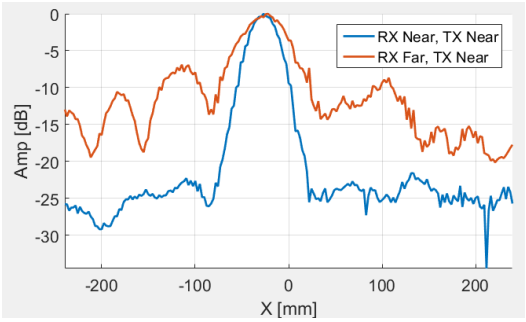

(a) The distance beampattern.

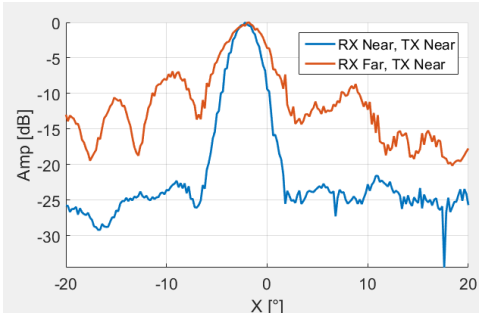

(b) The angle beampattern.

Figure 70 Comparison of receiver (RX) near and far field focusing for distance (left) and angle (right) beampatterns when the transmit signal is focusing near field.

Table 11 shows the key parameters of the experiment. Figure 68 shows the raw signal when near and far field receiver (RX) focusing with transmission (TX) focusing on the near field. Figure 69 shows the cross-correlation signal from the raw signal.

Figure 70 shows when the target is 300mm from the transmitting board and the transmitting signals TX near. The blue line is narrower than the red line. That means focusing the array in the near field can get more focusing results than only focusing the transmission in the near field.

4.5.2 The experiment data of 60kHz 300mm with TX far

Table 12 Key parameters of the experiment

Experiment serial number	Target distance(mm)	Transmitting signal frequency(kHz)	Transmitting signal type	Transmitting signal beamforming	Receiving signal beamforming
1.8	300	60	5-cycle sine waves	TX far	RX near
	300	60	5-cycle sine waves	TX far	RX far

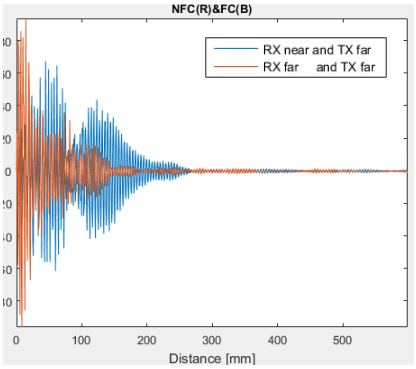

(a) The raw signal when array turned 20 degrees away from the rod.

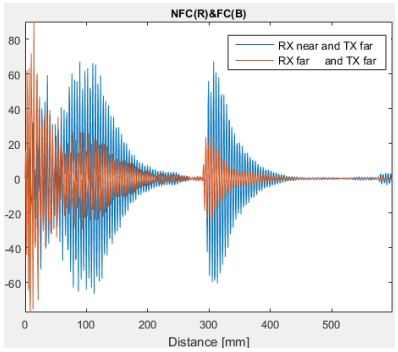

(b) The raw signal when array faced the rod.

Figure 71 Example raw signal when near and far field receiver (RX) focusing with transmission (TX) focusing on the far field. The left figure shows the array turned 20 degrees away from the rod. The right-side figure shows the array facing the rod. (60 kHz 300mm)

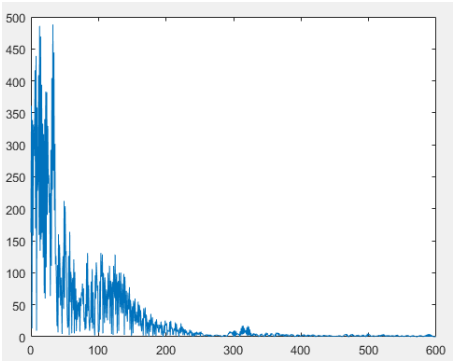

(a) The cross-correlation signal when array turned 20 degrees away from the rod.

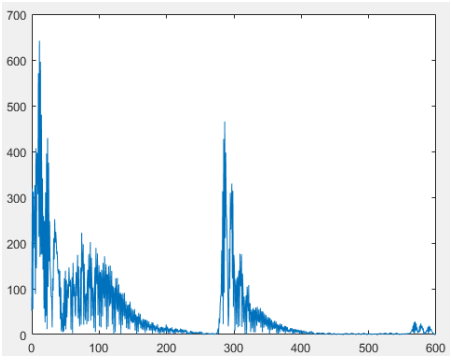

(b) The cross-correlation signal when array faced the rod.

Figure 72 The left figure shows the cross-correlation signal when the array is pointed away from the rod target. The right-side figure shows the cross-correlation signal when transmitting board is facing the target.

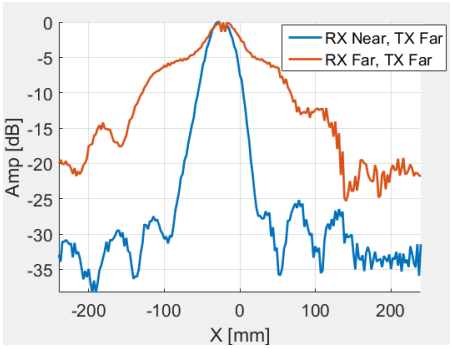

(a) The distance beampattern.

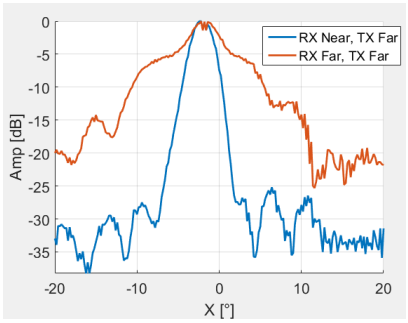

(b) The angle beampattern.

Figure 73 Comparison of receiver (RX) near and far field focusing for distance (left) and angle (right) beampatterns when the transmit signal is focusing far field.

Table 12 shows the key parameters of the experiment. Figure 71 shows the raw signal when near and far field receiver (RX) focusing with transmission (TX) focusing on the far field. Figure 72 shows the cross-correlation signal from the raw signal.

Figure 73 shows that when the target is 300mm away from the transmitting board and the transmitting signals are TX far, the blue line is narrower than the red line. That means focusing reception in the near field and transmission in the far field can get more focused results than focusing the array in the far field.

Comparing the graphics under two conditions, it can get the figure below:

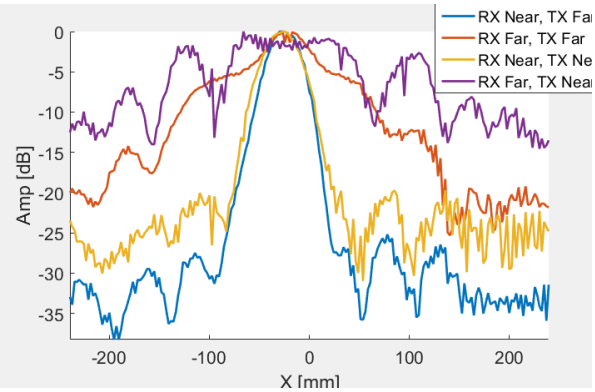

(a) The distance beampattern.

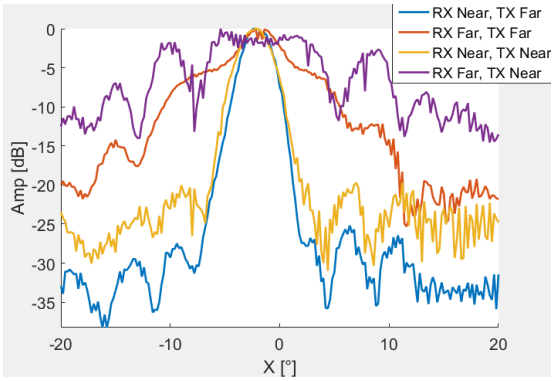

(b) The angle beampattern.

Figure 74 Combination of TX near and TX far curves at 60 kHz 300mm. (a)(b) stands for comparing in degree and millimetre.

Figure 74 shows that the yellow curve, which stands for TX near and RX near, and the blue curve for TX far and RX near, have a more focused result than the other two curves. Additionally, the purple curve and the red curve are approximately diverged. It cannot get accurate results from these curves compared to blue and yellow curves.

4.6 Summary

Figure 75 shows the curve combination of different reception and transmission focusing fields at 20 and 60 kHz when the target is 700mm from the array.

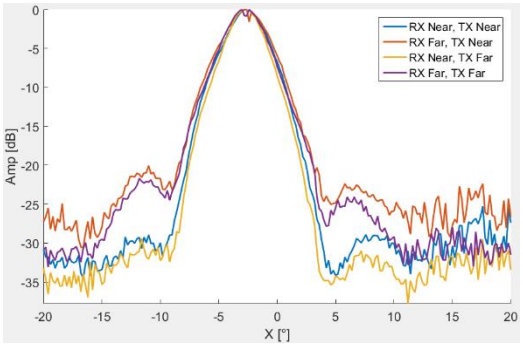

(a) Combination curves at 20 kHz when rod is at 700 mm.

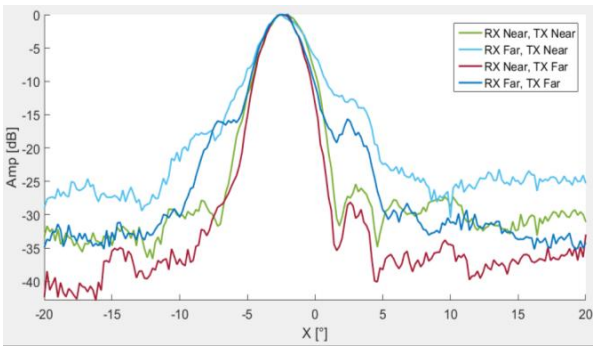

(b) Combination curves at 60 kHz when rod is at 700 mm.

Figure 75 Combination 20 kHz and 60 kHz curves when rod is at 700mm. (a) stands for RX near and far with TX near and far. (b) stands for RX near and far with TX near and far.

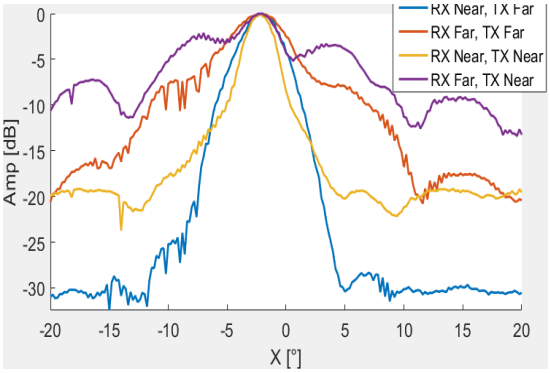

(a) Combination curves at 20 kHz when rod is at 300 mm.

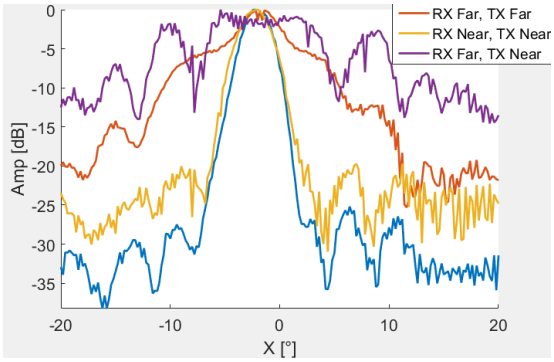

(b) Combination curves at 60 kHz when rod is at 300 mm.

Figure 76 Combination 20 kHz and 60 kHz curves when rod is at 300mm. (a) stands for RX near and far with TX near and far. (b) stands for RX near and far with TX near and far.

Figure 76 shows the curve combination of different reception and transmission focusing fields at 20 and 60 kHz when the target is 300mm from the array.

The initial assumption was that near-field focusing for transmission and reception would give optimal results since it provided the correct focus for beamforming. Far-field focusing was expected to give worse results, particularly as the reflecting object was brought closer to the array, due to the incorrect focusing being used for beamforming. It was seen to some extent. Near-field focusing of reception significantly improved in reduced beamwidth and dynamic range. However, limited improvement was seen for near-field focusing for transmission compared to far-field focusing. It may have been due to the limitations of the transmitter array PCB board, as will be discussed in the conclusion.

5. Pasture experiments

Some initial lab experiments were done using a grass sample obtained by cutting a section of grass with soil attached to investigate whether near-field and far-field focusing produced different results(Figure 77 and Figure 78). Two trials have been implemented at 20 and 60 kHz, but due to time constraints, only the trial of transmitting signals at 60 kHz has been shown here.

Table 13 Pasture sample experiments parameter

Experiment serial number	Focus distance(mm)	Transmitting signal frequency(kHz)	Transmitting signal type	Transmitting signal beamforming	Receiving signal beamforming
1.9	360	60	5-cycle sine waves	TX near	RX near
	360	60	5-cycle sine waves	TX far	RX near

Figure 77 A pasture sample with soil which is almost 400mmX400.

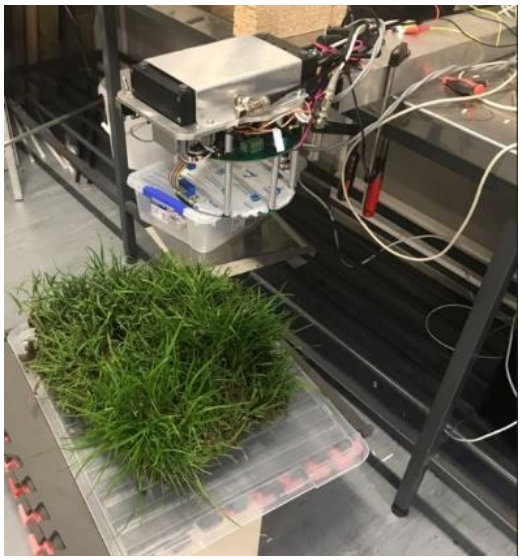

Figure 78 Set the transmitting and receiving system mounting onto the experimental table over the top of the pasture.

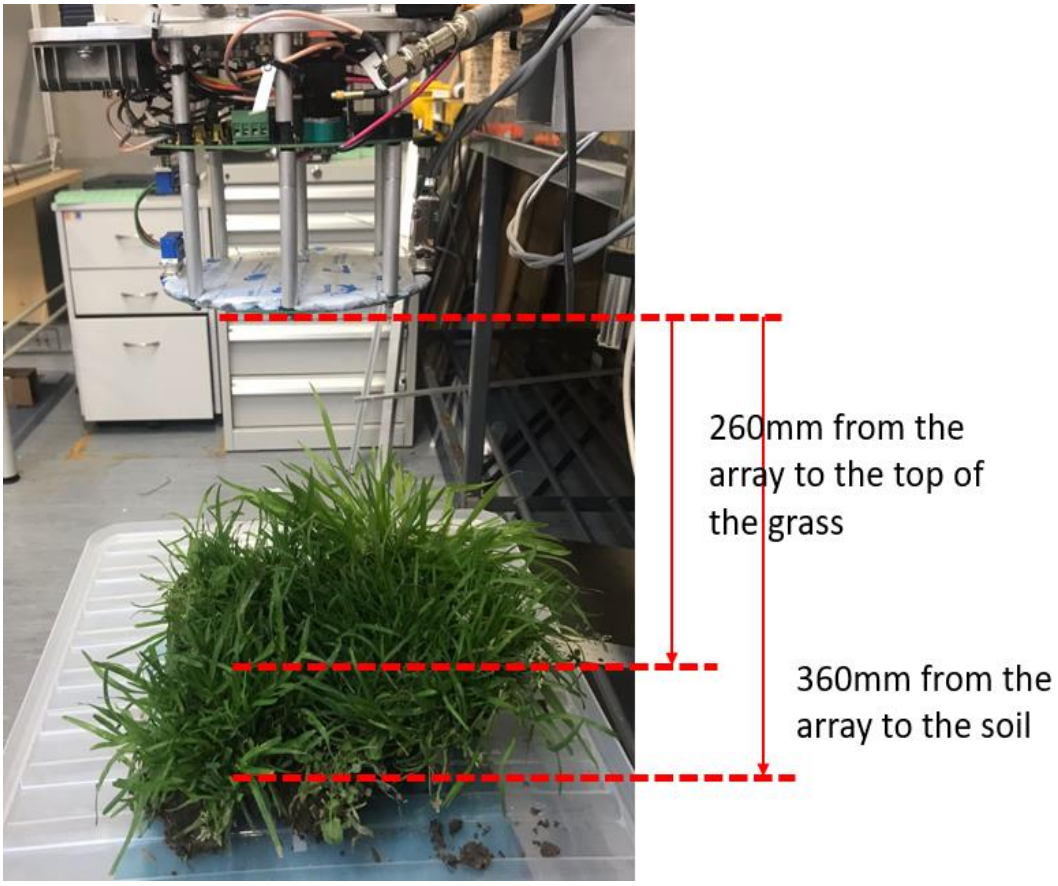

Figure 79 The distance from the soil to the board is about 360mm. The top of the grass is around 260mm.

Table 13 shows the key parameters of the experiment. Figure 77 shows the pasture example with soil. Figure 78 shows the setup. Table 13 Pasture sample experiments parameter

The array was positioned 360mm above the soil ground level of the pasture sample. The top of the grass was predominately located about 260mm below the array, with occasional leaves sticking out above this height at different positions to the side referred to in Figure 79.

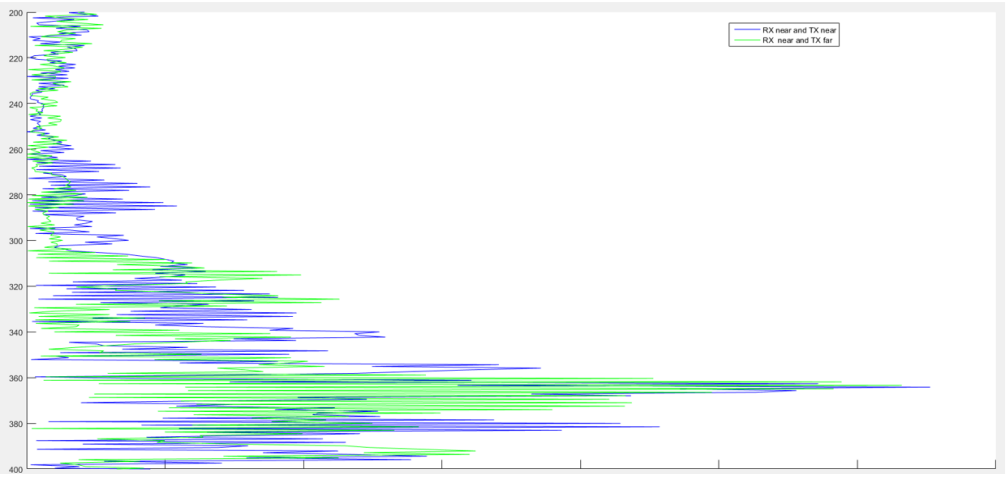

Figure 80 A sample of cross correlation signals of the same pasture at 60 kHz 360mm. Blue curve stands for RX near and TX near. Green curve stands for RX near and TX far.

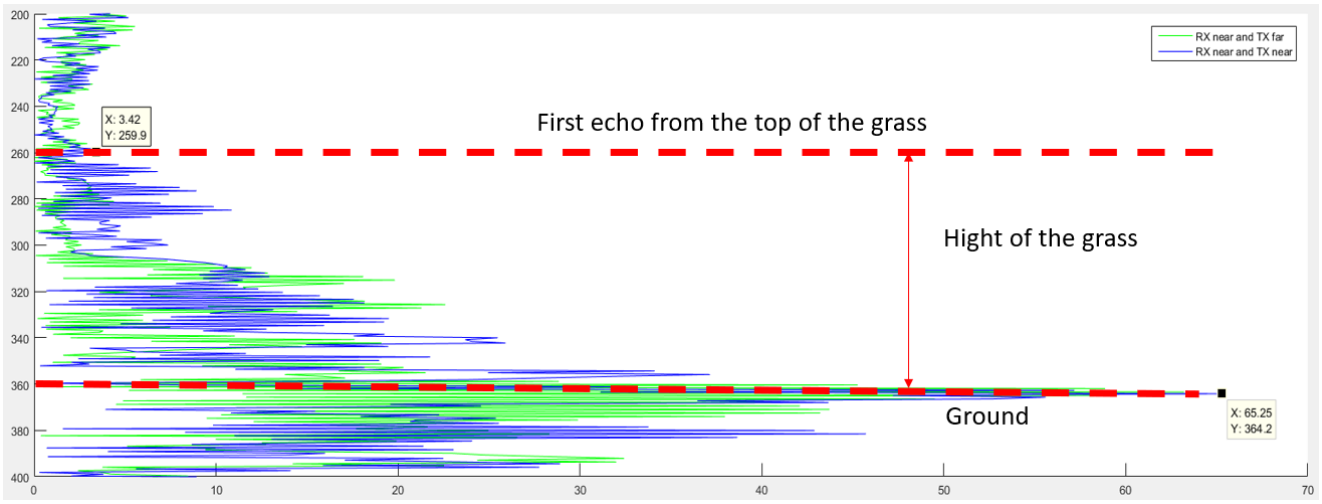

Figure 81 Green curves stand for RX near and TX near. Blue curves stand for RX near and TX far. Both curves are cross correlation signals at 60 kHz 360mm. Illustrate the position of ground and the top of the grass.

Figure 80 and Figure 81 show an example of the cross-correlation signal obtained from the pasture sample. The self-ringing of the transducers dominates the first part of the signal. It drops off about 240 mm from the array. It defines the minimum distance that an object can be detected reliably. At about 260mm, the signal increases again and peaks at 360 mm. These two distances correspond to the top of the grass and the ground positions, respectively.

The amplitude of the cross-correlation signal for the blue curve (RX near and TX near) is higher than the green curve (RX near and TX far) for the part of the signal corresponding to the echoes from the grass. Both lines have the same signal height, around 360mm, where the ground is. This result indicates that the near field focusing on transmission improved the ability to detect the grass. Far-field focusing for transmission struggled to pick up the top of the grass. It might indicate that near-field focusing is beneficial for pasture estimation. However, more work is needed to confirm this.

6. Conclusion

Legg and Bradley (Legg & Bradley, 2019b) developed an ultrasonic array for estimating pasture biomass. They used focusing of the array in the far field (focusing on a distance of infinity). The array could perform beamforming to focus the reception in the near field, although this was not done for pasture. However, due to the hardware configuration, the transmission system could not focus on the near field. The question was raised if improved pasture estimation performance could be achieved if the array was focused in the near-field.

This work extends on the work performed by Legg and Bradley by upgrading the transmitting system, allowing the transmitting to focus in the near field. This work included a 10-channel power amplifier system. However, these were not used due to the finding that the DACs used have enough power to drive the transmitting rings without the power amplifiers and that the power amplifier added extra noise.

The software was developed to allow the system to focus transmission and reception in the near field or far field. Measurements were made using a computer-controlled turntable system to measure the beam width of the arrays using different combinations of near and far field focusing for transmission and reception.

Table 14 ranks the array's performance regarding reduced beamwidth and dynamic range for different combinations of near and far field focusing for transmitting and receiving.

Table 14 Compare the experiment results in terms of beamwidth and dynamic range.

RX	TX	Focusing distance(mm)	Ranking(1=normal, 2=better, 3=best)
Near	Near	700	3
Near	Far	700	2
Far	Near	700	1
Far	Far	700	1
Near	Near	300	3
Near	Far	300	2
Far	Near	300	1
Far	Far	300	1

1. When receiving a signal focusing near field (RX near) and transmitting a signal focusing near field (TX near), the best signal resolution can be obtained.

2. When focusing the reception array in the near field and the transmission array in the far field, the signal resolution is second only to focusing the array in the near field.

In summary, it was found that focusing the receiver array in the near field significantly improved angular resolution and dynamic range (reduced side lobe levels), mainly when focusing on an object close to the array. However, focusing the transmission in the near-field had relatively little difference compared to far-field focusing.

The reduced efficiency of focusing for transmission may have been due to limitations in the transmission array hardware. It was found during experiments that transmission rings 2 and 3 near the array's centre were not working. It could potentially be due to an electrical short on the PCB. Additionally, the inner ring (ring 1) had little power due to having fewer transducers. It meant that the only rings efficiently working were on the outer part of the array. Could this have reduced the efficiency of the focus? Another potential cause could be the acoustic coupling of the transducer to the PCB board. When designing the array and simulating its performance, the assumption had been that the transducers produced a point sound source. However, could ultrasonic signals from the transducers propagate through the PCB, causing reduced focusing efficiency?

Initial experiments were performed on grass samples in the lab. From the cross-correlation signal curves comparing, focusing the transmitter and receiver array in the near field improved performance in detecting the grass, particularly the top of the grass, compared with focusing the receiver in the near field but also focusing the transmitter in the far field.

6.1 Future Work

More work could be performed to investigate why the transducer array did not show as much improvement for near-field focusing compared to far-field focusing as was expected in terms of beamwidth and dynamic range (reduction of sidelobe levels). It might be due to the only effective operating transducer rings being in the outer part of the array due to rings 2 and 3 not working and the design of the array.

Work could be done to see if the transmitter array could be repaired so that rings 2 and 3 could be used. Alternatively, a new transmitting board could be designed and built to have more transmission rings closer to the array's centre. In addition, investigations could be made into

whether the acoustic signals propagating through the PCB board affected the array's focusing ability and beam width. 10 channel rings need to be isolated to cut off the internal transmission path of the signal. Furthermore, since there is an interval between the transducers on each channel ring, these transducers are installed on a ring-shaped PCB board. If needed, consider isolating these transducers and only find a fulcrum on the back of the transducer to make it form a structure of 10 channel rings on a plane to cut off all internal transmission of signals, and then repeat the experiment to verify the theory. It is also something that can be done in the future.

More trials with pasture can be done in the lab and the wild field. What effect would pasture detection performance be if the transmitter and receiver arrays were focused in the far field and the array moved to 700mm above the pasture? Also, what effect would use 20 kHz instead of 60 kHz have? How do these compare with chirp? Also, trials should be performed in the field with the array mounted onto a farm vehicle, and what results would be obtained?

Another possible application of this work is to scan grapes to obtain their shape and quantity using 3D imaging technology.

Bibliography

Adamchuk, V. I., Rossel, R. V., Sudduth, K. A., & Lammers, P. S. (2011). Sensor fusion for precision agriculture. *Sensor fusion-foundation and applications*, 27-40.

Ahamed, T., Tian, L., Zhang, Y., & Ting, K. (2011). A review of remote sensing methods for biomass feedstock production. *Biomass and bioenergy, 35*(7), 2455-2469.

Ahmad, R., Kundu, T., & Placko, D. (2005). Modeling of phased array transducers. *The Journal of the Acoustical Society of America, 117*(4), 1762-1776.

Akhbari, S., Sammoura, F., Eovino, B., Yang, C., & Lin, L. (2016). Bimorph piezoelectric micromachined ultrasonic transducers. *Journal of Microelectromechanical Systems, 25*(2), 326-336.

Akhtar, A. M., Qazi, W. A., Ahmad, S. R., Gilani, H., Mahmood, S. A., & Rasool, A. (2020). Integration of high-resolution optical and SAR satellite remote sensing datasets for aboveground biomass estimation in subtropical pine forest, Pakistan. *Environmental Monitoring and Assessment, 192*, 1-17.

Ali, I., Cawkwell, F., Dwyer, E., & Green, S. (2016). Modelling managed grassland biomass estimation by using multitemporal remote sensing data—A machine learning approach. *IEEE Journal of Selected Topics in Applied Earth Observations and Remote Sensing, 10*(7), 3254-3264.

Allevato, G., Rutsch, M., Hinrichs, J., Haugwitz, C., Müller, R., Pesavento, M., & Kupnik, M. (2022). Air-coupled ultrasonic spiral phased array for high-precision beamforming and imaging. *IEEE Open Journal of Ultrasonics, Ferroelectrics, and Frequency Control, 2*, 40-54.

Brisco, B., Brown, R., Hirose, T., McNairn, H., & Staenz, K. (1998). Precision agriculture and the role of remote sensing: a review. *Canadian Journal of Remote Sensing, 24*(3), 315-327.

Buckley, K. (1987). Spatial/spectral filtering with linearly constrained minimum variance beamformers. *IEEE Transactions on Acoustics, Speech, and Signal Processing, 35*(3), 249-266.

Chen, J. C., Yao, K., & Hudson, R. E. (2002). Source localization and beamforming. *IEEE Signal Processing Magazine, 19*(2), 30-39.

Digilent. (2023). DT9836 manual. Retrieved from https://www.mccdaq.com/PDFs/Manuals/UM9836.pdf

Dworak, V., Selbeck, J., & Ehlert, D. (2011). Ranging sensors for vehicle-based measurement of crop stand and orchard parameters: a review. *Transactions of the ASABE, 54*(4), 1497-1510.

Earle, D., & McGowan, A. (1979). Evaluation and calibration of an automated rising plate meter for estimating dry matter yield of pasture. *Australian Journal of Experimental Agriculture, 19*(98), 337-343.

Enterprises, N. (2023, 2023). Pasture Reader. Retrieved from http://pasturereader.com.au/

Erdogan, H., Hershey, J. R., Watanabe, S., Mandel, M. I., & Le Roux, J. (2016). *Improved mvdr beamforming using single-channel mask prediction networks.* Paper presented at the Interspeech.

Fricke, T., & Wachendorf, M. (2013). Combining ultrasonic sward height and spectral signatures to assess the biomass of legume–grass swards. *Computers and Electronics in Agriculture, 99*, 236-247.

Gargiulo, J. I., Lyons, N. A., Masia, F., Beale, P., Insua, J. R., Correa-Luna, M., & Garcia, S. C. (2023). Comparison of Ground-Based, Unmanned Aerial Vehicles and Satellite Remote Sensing Technologies for Monitoring Pasture Biomass on Dairy Farms. *Remote Sensing, 15*(11), 2752.

Gomez Alvarez-Arenas, T. (2017). Air-coupled ultrasonic transducers. *Ultrasound in Food Processing: Recent Advances*, 175-228.

Hamid, U., Qamar, R. A., & Waqas, K. (2014). *Performance comparison of time-domain and frequency-domain beamforming techniques for sensor array processing.* Paper presented at the Proceedings of 2014 11th International Bhurban Conference on Applied Sciences & Technology (IBCAST) Islamabad, Pakistan, 14th-18th January, 2014.

Hardisky, M., Smart, R., & Klemas, V. (1983). Seasonal spectral characteristics and aboveground biomass of the tidal marsh plant. *Spartina-Alterniflora Photogrammetric Engineering and Remote Sensing, 49*, 85-92.

Harput, S., & Bozkurt, A. (2008). Ultrasonic phased array device for acoustic imaging in air. *IEEE Sensors Journal, 8*(11), 1755-1762.
Hutchings, N., Phillips, A., & Dobson, R. C. (1990). An ultrasonic rangefinder for measuring the undisturbed surface height of continuously grazed grass swards. *Grass and Forage Science, 45*(2), 119-127.
Instruments, T. (2013). Datasheet of integrated amplifier LM3886. Retrieved from https://www.ti.com/
Kažys, R., Vladišauskas, A., & Žukauskas, E. (2004). Wideband air–coupled ultrasonic transducers. *Ultragarsas/Ultrasound, 52*(3), 21-28.
Kumar, L., & Mutanga, O. (2017). Remote sensing of above-ground biomass. In (Vol. 9, pp. 935): MDPI.
Legg, M., & Bradley, S. (2019a). Ultrasonic Arrays for Remote Sensing of Pasture Biomass. *Remote Sensing, 12*, 111. doi:10.3390/rs12010111
Legg, M., & Bradley, S. (2019b). Ultrasonic arrays for remote sensing of pasture biomass. *Remote Sensing, 12*(1), 111.
Legg, M., & Bradley, S. (2019c). Ultrasonic Proximal Sensing of Pasture Biomass. *Remote Sensing, 11*(20), 2459. Retrieved from https://www.mdpi.com/2072-4292/11/20/2459
Legg, M., & Bradley, S. (2020). Ultrasonic Arrays for Remote Sensing of Pasture Biomass. *Remote Sensing, 12*(1), 111. Retrieved from https://www.mdpi.com/2072-4292/12/1/111
Liu, H., Bruning, B., Garnett, T., & Berger, B. (2020). Hyperspectral imaging and 3D technologies for plant phenotyping: From satellite to close-range sensing. *Computers and Electronics in Agriculture, 175*, 105621.
Lush, W. (1990). Turf growth and performance evaluation based on turf biomass and tiller density. *Agronomy Journal, 82*(3), 505-511.
Matrone, G., Ramalli, A., D'hooge, J., Tortoli, P., & Magenes, G. (2019). A comparison of coherence-based beamforming techniques in high-frame-rate ultrasound imaging with multi-line transmission. *IEEE transactions on ultrasonics, ferroelectrics, and frequency control, 67*(2), 329-340.
Milsom, A., Bell, O., Bailey, K., Brown, S. C., Barton, R. A., Moreno García, C., . . . Eady, C. C. (2019). *Assessing the ability of a stationary pasture height sensing device to estimate pasture growth and biomass*.
Neurochrome. (2023). Neurochrome Home page. Retrieved from https://neurochrome.com/collections/power-amplifiers/products/lm3886-done-right
Nordebo, S., Claesson, I., & Nordholm, S. (1994). Adaptive beamforming: spatial filter designed blocking matrix. *IEEE Journal of Oceanic Engineering, 19*(4), 583-590.
Omia, E., Bae, H., Park, E., Kim, M. S., Baek, I., Kabenge, I., & Cho, B.-K. (2023). Remote sensing in field crop monitoring: A comprehensive review of sensor systems, data analyses and recent advances. *Remote Sensing, 15*(2), 354.
Paul, Y., Barthez, D., Léveillé, R., Peter, V., & Scrivani, D. (1997). Side lobes and grating lobes artifacts in ultrasound imaging. *Veterinary Radiology & Ultrasound, 38*(5), 387-393.
Price, A., & Long, B. (2018). *Fibonacci spiral arranged ultrasound phased array for mid-air haptics.* Paper presented at the 2018 IEEE International Ultrasonics Symposium (IUS).
Qian, J., He, Z., Zhang, W., Huang, Y., Fu, N., & Chambers, J. (2018). Robust adaptive beamforming for multiple-input multiple-output radar with spatial filtering techniques. *Signal Processing, 143*, 152-160.
Reusch, S. (2009). Use of ultrasonic transducers for on-line biomass estimation in winter wheat. *Precision agriculture, 9*, 169-175.
Sherline. (2023). Retrieved from https://sherline.com/wp-content/uploads/2015/12/8700inst.pdf?_ga=2.160294335.346486135.1693506863-804959129.1693506863

Van Veen, B. D., & Buckley, K. M. (1988). Beamforming: A versatile approach to spatial filtering. *IEEE assp magazine, 5*(2), 4-24.

Wachendorf, M., Fricke, T., & Möckel, T. (2018). Remote sensing as a tool to assess botanical composition, structure, quantity and quality of temperate grasslands. *Grass and Forage Science, 73*(1), 1-14.

White, J. W., Andrade-Sanchez, P., Gore, M. A., Bronson, K. F., Coffelt, T. A., Conley, M. M., . . . Hunsaker, D. J. (2012). Field-based phenomics for plant genetics research. *Field Crops Research, 133*, 101-112.

Xiong, W., He, Q., & Peng, Z. (2020). Fibonacci array-based focused acoustic camera for estimating multiple moving sound sources. *Journal of Sound and Vibration, 478*, 115351.

You, W., Cretu, E., Rohling, R., & Cai, M. (2011). Tiltable ultrasonic transducers: Concept, beamforming methods and simulation. *IEEE Sensors Journal, 11*(10), 2286-2300.

Appendix A: Matlab code for beamwidth measurements

```
 clc; clear all; %close all;
ang0       = 20;
for txNo = 0;%1:-1:0
   DoTxNear = txNo;
   angles     = -20:0.2:20;
   TXCh = [0 0 0 0 0 0 0 0 0 0];
   TXCh(4:10) = 1;
   %TXCh(4) = 1;
   ground     = 300*1e-3; % This is the height in meters where the ground appears to be in the reflections of v1.
   fo         =  60e3;                    % Frequency [kHz].
   nAv        = 1;

   SoundOut       = ['pulse_',num2str(fo),'Hz'];%,'chirp'; % 'pulse_35kHz','tone_20_35kHz'
   C = clock;
   dateStr = [num2str(C(1)),num2str(C(2)),num2str(C(3))];
   fpath = ['./data/Not_Tx_Focused/Dist_',num2str(ground*1e3),'mm_',SoundOut,'/',dateStr];

   if ~exist(fpath,'dir'), mkdir(fpath); end

   % Trigger excitation board and ADC board should be, by default, the first one in the
   RecBoardNam  = 'DT9836(02)-3';
   TrigBoardNam = 'DT9836(01)-3';
   NamesOrdered = {'DT9836(02)-3','DT9836(01)-3','DT9832A(01)-3', 'DT9832A(00)-3', 'DT9836(00)-3'};
   boards     = daqhwinfo('dtol','BoardNames');

   boardNo = zeros(size(NamesOrdered));
   for m = 1:length(NamesOrdered)
      for k = 1:length(boards)
         if strcmp(boards{k},NamesOrdered{m})
            boardNo(m) = k-1;
         end
      end
   end

   for k = 1:length(boards)
      if strcmp(boards{k},TrigBoardNam)
         TrigBoard = k-1;
      end

   end

   for k = 1:length(boards)
      if strcmp(boards{k},RecBoardNam)
         RecBoard = k-1;
      end

   end

   %=========================================
   daqreset;
   if (~isempty(daqfind)), stop(daqfind); end
   try
      daqregister('dtol');                % Register DAQ Adaptor for MATLAB
   catch
      disp('ERROR: Cannot register the DAQ Adaptor for MATLAB!');
      return;
   end
   boards     = daqhwinfo('dtol');
   %=========================================================================
   %=========================================
   dio           = digitalio('dtol',TrigBoard); % Need to check correct board is selected.
   dCh            = 1:3;
   hline          = addline(dio, 15+dCh, 'Out'); % First digital out channel is 16.

   putvalue(dio.Line(1),1); % Set initial trigger signal to zero.

   %=========================================================================
   % Setup analogue input
   c             = 340;
   RecTime        = 2*ground*2/340; % Record time
   Fs             = 225e3;     % Sample rate
   NoSampPerTrig   = floor(RecTime*Fs);
```

```
N               = NoSampPerTrig;
TrigType_ai     = 'HwDigital';%'Immediate';%
LogMode         = 'Memory'; %'Disk';%'Disk&Memory'; %

Fso             = 500e3; %225e3; % Analogue output sampling frequency
TrigType_ao     = 'HwDigital'; %'Immediate'; %
WaitTime        = 10;
N_ao            = floor(RecTime*Fso);


ai          = analoginput('dtol', RecBoard ); %TrigBoard
Fs          = setverify(ai, 'SampleRate', Fs);  % Sets the sampling frequency. It returns the actual sampling frequency used by matlab.
addchannel(ai, 0:11) % Need to check that second board is the DT9832A and first board is DT9836;

set(ai,'TriggerType',       TrigType_ai,'SamplesPerTrigger',       NoSampPerTrig,       'LoggingMode',       LogMode,       'BufferingMode',
'Manual','BufferingConfig', [NoSampPerTrig 2]);     % Set parameters

TriggerCond = 'RisingEdge'; %'FallingEdge' 'RisingEdge'
%TriggerCondition = 'FallingEdge';
set(ai,'TriggerCondition',TriggerCond)    % Set parameters %FallingEdge%RisingEdge

%=========================================================================
%=========================================================================
% Analogue output set up

ao0     = analogoutput('dtol', boardNo(1));  % Construct analogue output object
addchannel(ao0, 0:1);
ao1     = analogoutput('dtol', boardNo(2));   % Construct analogue output object
addchannel(ao1, 0:1);
ao2     = analogoutput('dtol', boardNo(3));   % Construct analogue output object
addchannel(ao2, 0:1);
ao3     = analogoutput('dtol', boardNo(4));   % Construct analogue output object
addchannel(ao3, 0:1);
ao4     = analogoutput('dtol', boardNo(5));   % Construct analogue output object
addchannel(ao4, 0:1);

ao = [ao0,ao1,ao2,ao3,ao4];%[ao0 ao1 ao2 ao3 ao4];

set(ao, 'BufferingMode', 'Auto', 'TriggerType', TrigType_ao);    % Set parameters max(N,2)
Fso_        = setverify(ao, 'SampleRate', Fso);          % Sets the sampling frequency. It returns the actual sampling frequency used by matlab.
pause(0.1)

set(ao,'TriggerCondition', 'RisingEdge');
%set(ao1,'TriggerCondition', 'RisingEdge');


%=======================================
A     = 7;
ncy   = 5;                      % Number of cycles.
tor   = ncy/fo;                 % Period of transmit signal.
tto   = (0:1/Fso:tor)';         % Time
Wh    = hamming(length(tto));       % Hamming window.
yyo   = A * Wh .* sin(2*pi*fo*tto); % Hamming windowed sin wave.

tgo   = (0:1/Fs:tor)';          % Time
Wgh    = hamming(length(tgo));       % Hamming window.
go   = A * Wgh .* sin(2*pi*fo*tgo); % Hamming windowed sin wave.


%=======================================

% Calculate delays to focus reception and, to some extent, transmission at the ground.
TxRing          = [9.0  31.0 36.4 41.8 47.3 52.8 58.3 63.8 69.4 75.0].*1e-3;          % Transducer ring radius
%TxAmpRing      = [mean(TxRing(1:5)) mean(TxRing(6:10))]; % Only have two amplifiers so can calculate the center of two sets of rings.

%dtRx           = (sqrt(RxRing.^2 + v.ground^2)-v.ground)./c;    dtRx = dtRx-min(dtRx);
%dnRx           = dtRx*v.Fs; % Number of samples to delay
dtTx           = -(ground-sqrt(TxRing.^2 + ground^2))./c;
dtTx           = dtTx-min(dtTx);
dnTx           = round(dtTx*Fso); % Number of samples to delay transmission channels.

%=======================================
Rm =  [15.0 20.3 25.7 31.0 36.4 41.8 47.3 52.8 58.3 63.8 69.4 75.0].*1e-3;
dtRm            = -(sqrt(Rm.^2+ground^2)-ground)/c;% Number of samples to shiftting receiving rings.
dtRm            = dtRm-min(dtRm);
```

```
dnRm            = round(dtRm*Fs); %Number of samples to delay receiving rings.


%=========================================================================
%add delay to analog signal in frequency domin
doFD = 1;

if ~doFD
   %=============================================
   % Frequency domain focusing
   % Now shift the transmit signal
   f    = ((0:(N_ao-1))/N_ao*Fso)';
   w    = 2*pi*f;
   %k    = w/c;
   NL   = find(f>(fo-15e3),1,'first');
   NH   = find(f>(fo+15e3),1,'first');
   %=========================================

   yyoo = zeros(N_ao,1);
   yyoo(1:length(yyo)) = yyo;
   Y    = fft(yyoo);
   ys   = zeros(N_ao,length(TxRing));
   for spNo = 1:length(TxRing)
      %Ys        = zeros(N,1);
      Ys = zeros(N_ao,1);
      Ys(NL:NH)   = Y(NL:NH).*exp(-1i*w(NL:NH)*dtTx(spNo));
      ys(:,spNo)  = 2*real(ifft(Ys));
   end

else

   %==========================
   No = floor(RecTime*Fso);
   to = 0:1/Fso:(No-1)/Fso;
   indx = (1:length(yyo))';

   yo0 = zeros(N_ao,2);
   yo1 = zeros(N_ao,2);
   yo2 = zeros(N_ao,2);
   yo3 = zeros(N_ao,2);
   yo4 = zeros(N_ao,2);


   if ~DoTxNear     % true == TX near ;  faulse == TX far
      dnTx = zeros(1,10);
   end
   %TX_str = 'TX Near';
   yo0((indx+dnTx(1)),1) = TXCh(1)*yyo;
   yo0((indx+dnTx(2)),2) = TXCh(2)*yyo;

   yo1((indx+dnTx(3)),1) = TXCh(3)*yyo;
   yo1((indx+dnTx(4)),2) = TXCh(4)*yyo;

   yo2((indx+dnTx(5)),1) = TXCh(5)*yyo;
   yo2((indx+dnTx(6)),2) = TXCh(6)*yyo;

   yo3((indx+dnTx(7)),1) = TXCh(7)*yyo;
   yo3((indx+dnTx(8)),2) = TXCh(8)*yyo;

   yo4((indx+dnTx(9)),1) = TXCh(9)*yyo;
   yo4((indx+dnTx(10)),2) = TXCh(10)*yyo;
   %       else
   %          %TX_str = 'TX Far';
   %          %yo0(:,1) = [yyo];
   %          yo0(indx,:) = [TXCh(1)*yyo TXCh(2)*yyo];
   %          yo1(indx,:) = [TXCh(3)*yyo TXCh(4)*yyo];
   %          yo2(indx,:) = [TXCh(5)*yyo TXCh(6)*yyo];
   %          yo3(indx,:) = [TXCh(7)*yyo TXCh(8)*yyo];
   %          yo4(indx,:) = [TXCh(9)*yyo TXCh(10)*yyo];
   %       end
   %=========================================================

end
%=========================================================================
%=========================================================================
```

```
DirStr      = 'ClockWise';
%DirStr     = 'AntClockWise';

StepsPerDeg = 28800/360; % 80 steps per degree.

yAv         = zeros(N,12);

%po = 0;
RMS_Far = zeros(size(angles));
RMS_Near = zeros(size(angles));
for p = 1:length(angles)

   %po= po+1
   angDif      = angles(p) - ang0;

   fnam = [fpath,'/data_angle',num2str(angles(p)),'deg.mat'];
   if angDif >0
      dir = 0;
   else
      dir = 1;
   end
   putvalue(dio.Line(2),dir); % Set initial trigger signal to zero.

   MoveDeg     = abs(angDif);
   nSteps      = round(MoveDeg*StepsPerDeg);
   for nn = 1:nSteps
      putvalue(dio.Line(3),0); % Set initial trigger signal to zero.
      putvalue(dio.Line(3),1); % Set initial trigger signal to zero.
   end
   pause(0.01)
   ang0        = angles(p);
   putvalue(dio.Line(2),0);
   putvalue(dio.Line(3),0);
   pause(0.01)

   %start triggering signal
   pi = 0;
   %while 1
   yAv = zeros(N,12);
   for avNo = 1:nAv

      putvalue(dio.Line(1),0); % Set initial trigger signal to zero.

      putdata(ao0, yo0);
      putdata(ao1, yo1);
      putdata(ao2, yo2);
      putdata(ao3, yo3);
      putdata(ao4, yo4);
      pause(0.01)
      %start(ao);
      start([ao,ai]);
      pause(0.01)
      putvalue(dio.Line(1),1);
      %putvalue(dio.Line(1),1); % Set initial trigger signal to zero.
      wait(ai,WaitTime);
      wait(ao,WaitTime);
      %getdata(ai);
      stop(ao)
      [yy, time]    = getdata(ai);
      % Calculate transmitting signals using recording sampling rate (not
      % transmit sampling rate for cross-correlation.

      for k = 1:12
         yy(:,k) = yy(:,k) - mean(yy(:,k));
         %if k>1
         %    yy(:,k) = zeros(N,1);
         %end
      end
      yAv       = yAv + yy;
   end
   %yAv       = yy;

   yyi    = zeros(N,length(Rm));
   indx_i    = 1:length(yAv);
```

```
        %Perform beamforming
        for m = 1:length(Rm)

            yyi(indx_i+dnRm(m),m) = yAv(:,m);

        end
        y = sum(yyi,2);

        d = c*time/2;
        indz = find((d>ground)&(d<ground+70e-3));

                figure(1)
                clf
                plot(d*1000,y(1:N))
                hold on

        y_far = sum(yy,2);
        RMS_far = sqrt(mean(y_far(indz).^2));
        RMS_near = sqrt(mean(y(indz).^2));

        RMS_Far(p) = RMS_far;
        RMS_Near(p) = RMS_near;

        axis tight
        set(gca,'FontSize',10)
        title('NFC(R)&FC(B)','FontSize',10)
        xlabel('Distance [mm]')
        %end

        yyxc  =  xcorr(y,go); %Focused
        yyxc  =  yyxc(end-N+1:end);
        yyxc  =  abs(yyxc);

        save(fnam,'yy','y','time','RMS_near','RMS_far');


    end
    x = 700*sind(angles);
    RMS_Neardb = 20*log10(RMS_Near); RMS_Neardb = RMS_Neardb - max(RMS_Neardb);
    RMS_Fardb = 20*log10(RMS_Far); RMS_Fardb = RMS_Fardb - max(RMS_Fardb);

    figure(2)
    hold all

    plot(x,RMS_Neardb,x,RMS_Fardb,'LineWidth',2)
    xlabel('X [mm]','FontSize',16)
    ylabel('Amp [dB]','FontSize',16)
    set(gca,'FontSize',16)
    axis tight
    grid
    %legend({['RX Near, ',TX_str],['RX Far, ',TX_str],['RX Near, ',TX_str],['RX Far, ',TX_str]})
    legend({'RX Near, TX Near','RX Far, TX Near','RX Near, TX Far','RX Far, TX Far'})

    figure(3)
    hold all

    plot(angles,RMS_Neardb,angles,RMS_Fardb,'LineWidth',2)
    xlabel('X [°]','FontSize',16)
    ylabel('Amp [dB]','FontSize',16)
    set(gca,'FontSize',16)
    axis tight
    grid
    %legend({['RX Near, ',TX_str],['RX Far, ',TX_str],['RX Near, ',TX_str],['RX Far, ',TX_str]})
    legend({'RX Near, TX Near','RX Far, TX Near','RX Near, TX Far','RX Far, TX Far'})
end
```

Published with MATLAB® R2015b

Appendix B: The Matlab code for pasture sample testing

```
clc; clear all; %close all;

    txNo = 1;
    DoTxNear = txNo;

    TXCh = [0 0 0 0 0 0 0 0 0 0];
    TXCh(1:10) = 1;
    %TXCh(4) = 1;

    ground      = 700*1e-3; % This is the height in meters where the ground appears to be in the reflections of v1.
    fo          =  20e3;                    % Frequency [kHz].
    nAv         = 1;

    SoundOut        = ['pulse_',num2str(fo),'Hz'];%,'chirp'; % 'pulse_35kHz','tone_20_35kHz'
    C = clock;
    dateStr = [num2str(C(1)),num2str(C(2)),num2str(C(3))];
    fpath = ['./data/Not_Tx_Focused/Dist_',num2str(ground*1e3),'mm_',SoundOut,'/',dateStr];

    if ~exist(fpath,'dir'), mkdir(fpath); end

    % Trigger excitation board and ADC board should be the first in the list by default.
    %%set default DT9836 board
    RecBoardNam  = 'DT9836(02)-3';
    TrigBoardNam = 'DT9836(01)-3';
    NamesOrdered = {'DT9836(02)-3','DT9836(01)-3','DT9832A(01)-3', 'DT9832A(00)-3', 'DT9836(00)-3'};
    boards      = daqhwinfo('dtol','BoardNames');

    boardNo = zeros(size(NamesOrdered));
    for m = 1:length(NamesOrdered)
       for k = 1:length(boards)
          if strcmp(boards{k},NamesOrdered{m})
             boardNo(m) = k-1;
          end
       end
    end

    for k = 1:length(boards)
       if strcmp(boards{k},TrigBoardNam)
          TrigBoard = k-1;
       end

    end

    for k = 1:length(boards)
       if strcmp(boards{k},RecBoardNam)
          RecBoard = k-1;
       end

    end

    %=========================================
    daqreset;
    if (~isempty(daqfind)), stop(daqfind); end
    try
       daqregister('dtol');                 % Register DAQ Adaptor for MATLAB
    catch
       disp('ERROR: Cannot register the DAQ Adaptor for MATLAB!');
       return;
    end
    boards      = daqhwinfo('dtol');
    %=========================================================================
    %=========================================
    dio             = digitalio('dtol',TrigBoard); % Need to check correct board is selected.
    dCh              = 1:3;
    hline           = addline(dio, 15+dCh, 'Out'); % First digital out channel is 16.

    putvalue(dio.Line(1),1); % Set initial trigger signal to zero.
```

```
%==========================================================================
```

```
Error using daqhwinfo (line 131)
Failure to find requested data acquisition device: dtol.

Error in grass (line 33)
    boards      = daqhwinfo('dtol','BoardNames');
```

Setup analogue input

```
    c               = 340;
    RecTime         = 2*ground*2/340; % Record time
    Fs              = 225e3;     % Sample rate
    NoSampPerTrig   = floor(RecTime*Fs);
    N               = NoSampPerTrig;
    TrigType_ai     = 'HwDigital';%'Immediate';%
    LogMode         = 'Memory'; %'Disk';%'Disk&Memory'; %

    Fso             = 500e3; %225e3; % Analogue output sampling frequency
    TrigType_ao     = 'HwDigital'; %'Immediate'; %
    WaitTime        = 10;
    N_ao            = floor(RecTime*Fso);


    ai          = analoginput('dtol', RecBoard ); %TrigBoard
    Fs          = setverify(ai, 'SampleRate', Fs);  % Sets the sampling frequency. It returns the actual sampling frequency used by matlab.
    addchannel(ai, 0:11) % Need to check that second board is the DT9832A and first board is DT9836;

    set(ai,'TriggerType',       TrigType_ai,'SamplesPerTrigger',       NoSampPerTrig,       'LoggingMode',       LogMode,       'BufferingMode',
'Manual','BufferingConfig', [NoSampPerTrig 2]);     % Set parameters

    TriggerCond = 'RisingEdge'; %'FallingEdge' 'RisingEdge'
    %TriggerCondition = 'FallingEdge';
    set(ai,'TriggerCondition',TriggerCond)    % Set parameters %FallingEdge%RisingEdge

    get(ai,'TriggerCondition')    % Set parameters

    %==========================================================================
    %==========================================================================
```

Analogue output set up

```
    ao0         = analogoutput('dtol', boardNo(1));   % Construct analogue output object
    addchannel(ao0, 0:1);
    ao1         = analogoutput('dtol', boardNo(2));   % Construct analogue output object
    addchannel(ao1, 0:1);
    ao2         = analogoutput('dtol', boardNo(3));   % Construct analogue output object
    addchannel(ao2, 0:1);
    ao3         = analogoutput('dtol', boardNo(4));   % Construct analogue output object
    addchannel(ao3, 0:1);
    ao4         = analogoutput('dtol', boardNo(5));   % Construct analogue output object
    addchannel(ao4, 0:1);

    ao = [ao0,ao1,ao2,ao3,ao4];%[ao0 ao1 ao2 ao3 ao4];

    set(ao, 'BufferingMode', 'Auto', 'TriggerType', TrigType_ao);    % Set parameters max(N,2)
    Fso_       = setverify(ao, 'SampleRate', Fso);          % Sets the sampling frequency. It returns the actual sampling frequency used by Matlab.
    pause(0.1)

    set(ao,'TriggerCondition', 'RisingEdge');
    %set(ao1,'TriggerCondition', 'RisingEdge');


    %=====================================
    A     = 7;
    if 1
        ncy   = 5;                      % Number of cycles.
        tor   = ncy/fo;                 % Period of transmit signal.
        tto   = (0:1/Fso:tor)';         % Time
        Wh    = hamming(length(tto));   % Hamming window.
        yyo   = A * Wh .* sin(2*pi*fo*tto); % Hamming windowed sin wave.


        tgo   = (0:1/Fs:tor)';          % Time
```

```
    Wgh    = hamming(length(tgo));      % Hamming window.
    go   = A * Wgh .* sin(2*pi*fo*tgo); % Hamming windowed sin wave.
  else
    tor = 0.5e-3;
    fo   = [20e3 35e3];
    %fo   = [50e3 70e3];
    tto    = (0:(1/Fso):tor)';
    Wh    = ones(size(tto));
    yyo =   A.*Wh.* chirp(tto,fo(1),tor,fo(2),'linear',90);

    tgo    = (0:(1/Fs):tor)';
    Wgh    = ones(size(tgo));
    go =   A.*Wgh.* chirp(tgo,fo(1),tor,fo(2),'linear',90);

  end



%=========================================
%Calculate delays to focus reception and, to some extent, transmission at the ground.

  TxRing         = [9.0  31.0 36.4 41.8 47.3 52.8 58.3 63.8 69.4 75.0].*1e-3;          % Transducer ring radius
  %TxAmpRing       = [mean(TxRing(1:5)) mean(TxRing(6:10))]; % Only have two amplifiers so can calculate center of two sets of rings.

  %dtRx           = (sqrt(RxRing.^2 + v.ground^2)-v.ground)./c;    dtRx = dtRx-min(dtRx);
  %dnRx           = dtRx*v.Fs; % Number of samples to delay
  dtTx           = -(ground-sqrt(TxRing.^2 + ground^2))./c;
  dtTx           = dtTx-min(dtTx);
  dnTx           = round(dtTx*Fso); % Number of samples to delay transmission channels.

  %=========================================
  Rm =  [15.0 20.3 25.7 31.0 36.4 41.8 47.3 52.8 58.3 63.8 69.4 75.0].*1e-3;
  dtRm             = -(sqrt(Rm.^2+ground^2)-ground)/c;% Number of samples to shiftting receiving rings.
  dtRm             = dtRm-min(dtRm);
  dnRm             = round(dtRm*Fs); %Number of samples to delay receiving rings.


  %=====================================================================
  %%add delay to analog signal in frequency domin
  doFD = 1;



  if ~doFD


    %================================================
    % Frequency domain focusing


    % Now shift the transmit signal
    f    = ((0:(N_ao-1))/N_ao*Fso)';
    w    = 2*pi*f;
    %k    = w/c;
    NL   = find(f>(fo-15e3),1,'first');
    NH   = find(f>(fo+15e3),1,'first');
    %=========================================



    yyoo = zeros(N_ao,1);
    yyoo(1:length(yyo)) = yyo;
    Y    = fft(yyoo);
    ys   = zeros(N_ao,length(TxRing));
    for spNo = 1:length(TxRing)
      %Ys         = zeros(N,1);
      Ys = zeros(N_ao,1);
      Ys(NL:NH)   = Y(NL:NH).*exp(-1i*w(NL:NH)*dtTx(spNo));
      ys(:,spNo)  = 2*real(ifft(Ys));
    end

  else
```

```
        %============================
        No = floor(RecTime*Fso);
        to = 0:1/Fso:(No-1)/Fso;
        indx = (1:length(yyo))';

        yo0 = zeros(N_ao,2);
        yo1 = zeros(N_ao,2);
        yo2 = zeros(N_ao,2);
        yo3 = zeros(N_ao,2);
        yo4 = zeros(N_ao,2);


        if DoTxNear
           yo0((indx+dnTx(1)),1) = TXCh(1)*yyo;
           yo0((indx+dnTx(2)),2) = TXCh(2)*yyo;

           yo1((indx+dnTx(3)),1) = TXCh(3)*yyo;
           yo1((indx+dnTx(4)),2) = TXCh(4)*yyo;

           yo2((indx+dnTx(5)),1) = TXCh(5)*yyo;
           yo2((indx+dnTx(6)),2) = TXCh(6)*yyo;

           yo3((indx+dnTx(7)),1) = TXCh(7)*yyo;
           yo3((indx+dnTx(8)),2) = TXCh(8)*yyo;

           yo4((indx+dnTx(9)),1) = TXCh(9)*yyo;
           yo4((indx+dnTx(10)),2) = TXCh(10)*yyo;
        else
           %TX_str = 'TX Far';
           %yo0(:,1) = [yyo];
           yo0(indx,:) = [TXCh(1)*yyo TXCh(2)*yyo];
           yo1(indx,:) = [TXCh(3)*yyo TXCh(4)*yyo];
           yo2(indx,:) = [TXCh(5)*yyo TXCh(6)*yyo];
           yo3(indx,:) = [TXCh(7)*yyo TXCh(8)*yyo];
           yo4(indx,:) = [TXCh(9)*yyo TXCh(10)*yyo];
        end
        %============================================================


    end

    %=====================================================================

    %=====================================================================
    DirStr     = 'ClockWise';
    %DirStr     = 'AntClockWise';

    StepsPerDeg = 28800/360; % 80 steps per degree.

    yAv        = zeros(N,12);

    %po = 0;
%    RMS_Far = zeros(size(angles));
%    RMS_Near = zeros(size(angles));
%    for p = 1:length(angles)
%
%        %po= po+1
%        angDif      = angles(p) - ang0;
%
%        fnam = [fpath,'/data_angle',num2str(angles(p)),'deg.mat'];
%        if angDif >0
%           dir = 0;
%        else
%           dir = 1;
%        end
%        putvalue(dio.Line(2),dir); % Set initial trigger signal to zero.
%
%        MoveDeg     = abs(angDif);
%        nSteps      = round(MoveDeg*StepsPerDeg);
%        for nn = 1:nSteps
%           putvalue(dio.Line(3),0); % Set initial trigger signal to zero.
%           putvalue(dio.Line(3),1); % Set initial trigger signal to zero.
%        end
%        pause(0.01)
%        ang0        = angles(p);
%        putvalue(dio.Line(2),0);
```

```
%       putvalue(dio.Line(3),0);
%       pause(0.01)

%while 1;
if 1
    %start triggering signal
    pi = 0;
    %while 1
    yAv = zeros(N,12);
    for avNo = 1:nAv
       %pi=pi+1
       %=======================


       putvalue(dio.Line(1),0); % Set initial trigger signal to zero.

       %pause(0.02)
       putdata(ao0, yo0);
       putdata(ao1, yo1);
       putdata(ao2, yo2);
       putdata(ao3, yo3);
       putdata(ao4, yo4);
       pause(0.01)
       %start(ao);
       start([ao,ai]);
       pause(0.01)
       putvalue(dio.Line(1),1);
       pause(0.1)
       %putvalue(dio.Line(1),1);
       %pause(0.1)
       %putvalue(dio.Line(1),0);
       %putvalue(dio.Line(1),1); % Set initial trigger signal to zero.
       pause(0.5)
       wait(ai,WaitTime);
       wait(ao,WaitTime);
       %getdata(ai);
       stop(ao)
       %stop([ao,ai]); %ao,
       %pause(0.1)
       [yy, time]    = getdata(ai);




       for k = 1:12
          yy(:,k) = yy(:,k) - mean(yy(:,k));
          %if k>1
          %    yy(:,k) = zeros(N,1);
          %end
       end
       yAv      = yAv + yy;
    end
    %yAv      = yy;

    yyi    = zeros(N,length(Rm));
    indx_i    = 1:length(yAv);

    %Perform beamforming
    for m = 1:length(Rm)

       yyi(indx_i+dnRm(m),m) = yAv(:,m);

    end

    d = c*time/2;
    indz = find((d>ground)&(d<ground+70e-3));

     y_far = sum(yy,2);

%       figure(1)
%            clf
%            plot(d*1000,y(1:N),d*1000,y_far(1:N))
%            hold on
```

```
%       RMS_far = sqrt(mean(y_far(indz).^2));
%       RMS_near = sqrt(mean(y(indz).^2));
%
%       RMS_Far(p) = RMS_far;
%       RMS_Near(p) = RMS_near;
      %        whos RMS_Far RMS far

      %        plot(d*1000,y_far) %d(indz)*1000,y_far(indz),'r'


      %
%       axis tight


      %yyxc  =  xcorr(y_far,go);
      yyxc  =  xcorr(y,go); %Focused
      yyxc  =  yyxc(end-N+1:end);
      yyxc  =  abs(yyxc);

      [val,indx] = max(yyxc);
      %yyxc = yyxc/val;



      %yyxc  =  20*log10(yyxc);

      yyxc_f  =  xcorr(y_far,go); %Focused
      yyxc_f  =  yyxc_f(end-N+1:end);
      yyxc_f  =  abs(yyxc_f);
      [val,indx] = max(yyxc_f);

            figure(5)

            hold all
            %plot(yyxc,d*1000,'b') % Near
            %plot(yyxc_f,d*1000,'r');
            %plot(yyxc,d*1000,'g') % Near
            plot(yyxc_f,d*1000,'m');
            ylim([200 400])
            set(gca,'Ydir','reverse')


    %   save(fnam,'yy','y','time','RMS_near','RMS_far');


      %end
   end
```

Published with MATLAB® R2015b